COMPLEMENTING SELF-CONSISTENCY WITH CROSS-MODEL DISAGREEMENT FOR UNCERTAINTY QUANTIFICATION

Kimia Hamidieh[1]*, **Veronika Thost**[2], **Walter Gerych**[3†], **Mikhail Yurochkin**[4‡], **Marzyeh Ghassemi**[1]

[1]MIT [2] MIT-IBM Watson AI Lab [3]WPI, [4] IFM MBZUAI

ABSTRACT

Large language models (LLMs) often produce confident yet incorrect responses, and uncertainty quantification is one potential solution to more robust usage. Recent works routinely rely on self-consistency to estimate aleatoric uncertainty (AU), yet this proxy collapses when models are overconfident and produce the same incorrect answer across samples. We analyze this regime and show that cross-model semantic disagreement is higher on incorrect answers precisely when AU is low. Motivated by this, we introduce an epistemic uncertainty (EU) term that operates in the black-box access setting: EU uses only generated text from a small, scale-matched ensemble and is computed as the gap between inter-model and intra-model sequence-semantic similarity. We then define total uncertainty (TU) as the sum of AU and EU. In a comprehensive study across five 7–9B instruction-tuned models and ten long-form tasks, TU improves ranking calibration and selective abstention relative to AU, and EU reliably flags confident failures where AU is low. We further characterize when EU is most useful via agreement and complementarity diagnostics.

1 INTRODUCTION

Reliable uncertainty estimates are a prerequisite for deploying large language models (LLMs) in high-stakes domains (Chakraborti et al., 2025). Many existing approaches for LLM uncertainty estimation are based on model's *self*-confidence (Xia et al., 2025; Vashurin et al., 2025; Shorinwa et al., 2024), such as by measuring response consistency under sampling (Kuhn et al., 2023a; Lin et al., 2023; Nikitin et al., 2024; Aichberger et al., 2024) or querying for a verbalized uncertainty score (Lin et al., 2022). These metrics capture how internally confident a model is in its prediction – a notion of *predictive aleatoric uncertainty* (AU). But this leaves an important question unanswered: how confident should *we* be in the model? A model might be *confident but wrong*, such as responding with the same incorrect answer with high probability (see Figure 1). In these cases, methods that rely on self-consistency can fail (Kossen et al., 2024). To address this, we focus on estimating *epistemic uncertainty* (EU) – uncertainty in our *choice* of model – which better reflects whether a model's confidence is trustworthy for a given input.

Estimating EU requires evaluating a distribution of plausible models, which is prohibitively costly for LLMs, as training even one additional model adds significant overhead (Kirsch, 2024; Cottier et al., 2024). Recent shortcuts approximate EU in logit space (Ma et al., 2025), inject Bayesian noise during decoding (Liu et al., 2025; Gao et al., 2024), or rely on verifier–model disagreement (Xue et al., 2025), but each imposes strong task or architecture-specific assumptions. We instead capitalize on the ecosystem of open-weight LLMs: sampling responses from a small, scale-matched ensemble lets us estimate EU directly from cross-model semantic disagreement, without additional training. While prior work has shown that LLM ensembles can improve accuracy (Lu et al., 2024; Dey et al., 2025; Chen et al., 2025; Shnitzer et al., 2023; Ielanskyi et al.), their use for uncertainty quantification has not been systematically explored.

*Correspondence to hamidieh@mit.edu.
† Work done while at MIT. ‡ Work done while at the MIT-IBM Watson AI Lab.

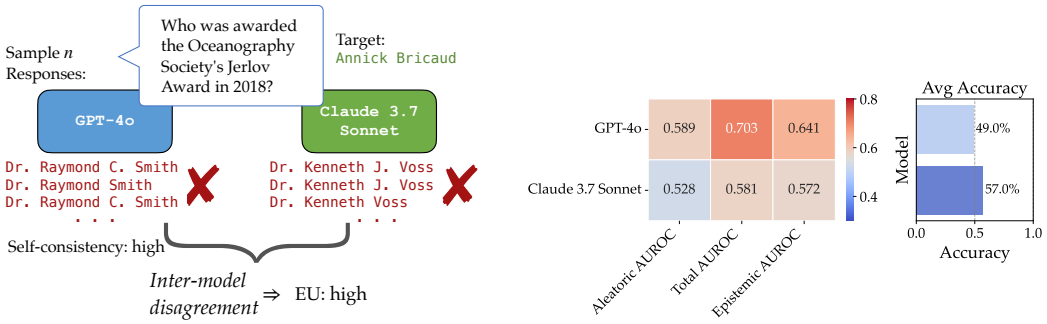

Figure 1: (a) Two models confidently produce distinct, incorrect answers to a factual question, which results in low intra-model variability (AU) but high semantic disagreement across models (EU). (b) Total uncertainty (TU = AU + EU) effectively improves uncertainty calibration with correcness in terms of AUROC on `SimpleQA`.

By enabling scalable estimation of EU from model outputs alone, we can combine it with AU to obtain a more robust measure of uncertainty, Total Uncertainty (TU). These two forms of uncertainty are complementary; AU reflects variability in a model's own predictions, while EU measures divergence from other plausible models (Schweighofer et al., 2023). Together, they allow TU to account for both internal inconsistency and external disagreement.

We evaluate EU, AU and TU on two standard axes: ranking-based calibration (via AUROC) and selective prediction (via abstention under uncertainty thresholds), across a range of models and generation tasks. We conduct comprehensive experiments across five 7–9B parameter Instruction-tuned models (Yang et al., 2024; Jiang et al., 2023; Grattafiori et al., 2024; Granite Team, 2024), on *ten* long-form generation tasks spanning QA, summarization, translation, and math reasoning (Joshi et al., 2017; Yang et al., 2018; Narayan et al., 2018). We also repeat these experiments for API models such as `GPT-4o` (Hurst et al., 2024) and `Claude 3.7 Sonnet` (Claude) on `SimpleQA` (Wei et al., 2024). Our contributions are as follows:

- We diagnose the failure mode of self-consistency as an aleatoric proxy: it often collapses on *confident errors*, or prompts where the model produces the same wrong answer repeatedly.
- We introduce an epistemic term based on cross-model semantic disagreement within a small, scale-matched ensemble, and show that it reliably identifies confident but incorrect responses.
- We conduct an extensive empirical study across ten long-form generation tasks and five reference models, and show that TU consistently outperforms AU in both AUROC and selective abstention.
- We show that the proposed EU is most informative in tasks with a unique correct answer, such as factual QA and translation.

2 Related Works

Aleatoric Uncertainty in LLMs. Existing approaches mainly focus on AU, which captures response inconsistency or input ambiguity. Recent surveys provide extensive reviews of these methods (Xia et al., 2025; Shorinwa et al., 2024; Vashurin et al., 2025). Typical strategies involve sampling multiple responses per prompt and analyzing their semantic consistency, often through clustering or entropy-based metrics (Lin et al., 2023). In line with prior evaluations, we adopt degree-based semantic dispersion (Lin et al., 2023) as the AU baseline used throughout this paper.

Bayesian-inspired EU Estimation. A line of research employs Bayesian-inspired methods, such as adding noise to embeddings during generation to approximate uncertainty in model weights (Liu et al., 2025), sampling from a model with different temperatures (Gao et al., 2024), or leverage entropy from decoding from different hidden states as proxy for uncertainty, which provides a computationally efficient alternative to exhaustive sampling (Gao et al., 2025). Training ensembles explicitly, such as LoRA-based methods (Wang et al., 2023), demonstrate improved uncertainty calibration but incur significant computational costs. Another work (Ma et al., 2025) calculates AU and EU on token level by considering the LLM logits as parameters of a Dirichlet distribution and by applying other UQ methods subsequently. Unlike approaches that require logits or hidden states, whereas our estimator operates only on generated text (Eq. 3), which enables application to black-box models.

Prompt-Based and Verifier-Based EU Estimation. Prior works in iterative prompting (Abbasi Yadkori et al., 2024; Johnson et al., 2024) estimate epistemic uncertainty by iteratively querying the same model, adding previous responses to the later queries' prompts, and measuring probabilistic inconsistencies. However, these methods have limitations: gains over AU are mainly reported on multi-label data, with limited benefits on standard single-label QA (Abbasi Yadkori et al., 2024), and some are evaluated only on synthetic data (Johnson et al., 2024). Xue et al. (2025) utilizes one verifier LLM and shows that inter-model disagreement as a proxy for EU complements AU in cases where we reach the performance bounds of self-consistency. Their practical rule triggers cross-consistency only at intermediate AU, whereas our evaluation, and (Simhi et al., 2025), indicates that low AU is especially prone to hallucination and is best complemented by EU (Sec. 5.1). Prior works are mostly limited to special kinds of question-answering data, do not account for the impact of the vast LLM model space on EU, and do not fully explore interactions between AU and EU, gaps our work addresses explicitly.

LLM Ensembles. Our work builds upon classical uncertainty estimation, such as deep and dropout ensembles (Lakshminarayanan et al., 2017; Gal & Ghahramani, 2016) and is closely related to LLM ensemble applications (Lu et al., 2024). In particular, various recent works focus on LLM collaborations (Dey et al., 2025), verifier LLMs (Lifshitz et al., 2025), and sampling from multiple LLMs (Chen et al., 2025). We study LLM ensembles from the viewpoint of uncertainty estimation.

3 Quantifying Predictive Uncertainty Using Response Similarity

Let ω be the particular parameterization of an LLM, and let x be a prompt. Our goal is to quantify the predictive uncertainty of ω given x as input. As is standard, we categorize predictive uncertainty into two components: AU and EU (Hüllermeier & Waegeman, 2021). The aleatoric component captures the inherent unpredictability of the response to x under the model ω, while the epistemic component captures our uncertainty in ω being the correct parametrization to use when responding to input x. We define total predictive uncertainty additively as the sum of the aleatoric and epistemic uncertainties.

3.1 Aleatoric Uncertainty via Intra-Model Response Similarity

Many recent works have proposed techniques to measure the randomness in LLM responses (Kuhn et al., 2023b; Lin et al., 2023; Liu et al., 2024). These techniques typically focus on measures of *semantic* uncertainty, where uncertainty is defined as a function of how often an LLM produces semantically distinct outputs given the same input (Kuhn et al., 2023b; Lin et al., 2023). In particular, Lin et al. (2023) propose a measure equivalent to[1] the following:

$$U_{\text{aleatoric}}(x;\omega) = \mathbb{E}_{r_1^\omega \sim p(\cdot|x,\omega)} \mathbb{E}_{r_2^\omega \sim p(\cdot|x,\omega)} \left[1 - s(r_1^\omega, r_2^\omega)\right], \tag{1}$$

where $s(\cdot,\cdot)$ is a similarity metric for responses such as the cosine similarity in an embedding space.

In essence, Equation 1 corresponds to the expected similarity between two responses independently sampled from $p(\cdot|x,\omega)$, the response distribution of ω conditioned on x. If responses typically have the same semantic meaning as each other, meaning that the meaning of the response does not vary when resampled, then $U_{\text{aleatoric}}(x;\omega)$ will be close to 0, which means that there is little uncertainty in how ω will respond to x. If the model is likely to produce semantically distinct responses for the same input, then $U_{\text{aleatoric}}(x;\omega)$ will be high, which means ω has high uncertainty for x.

Equation 1 captures the inherent uncertainty in the response to x given model ω. However, ω may not be the optimal model to use for x, and Equation 1 fails to capture the inherent uncertainty that comes from choosing ω as our parameterization. There is thus a need to also capture the *epistemic* uncertainty that comes from our model choice.

3.2 Epistemic Uncertainty as Inter-Model Response Similarity

Let ω^* represent a hypothetical "ideal" model, such that $p(\cdot|x;\omega^*) = p(\cdot|x)$; the distribution of responses from ω^* equals the true response distribution. We can thus quantify the epistemic

[1]This is equivalent to U_{Deg} in Lin et al. (2023).

uncertainty of ω as a divergence between ω and ω^*; e.g., $U_{\text{epistemic}}(x, \omega) = D(\omega \,||\, \omega^*)$ (Schweighofer et al., 2023). We define D as follows:

$$D(\omega \,||\, \omega^*) = -\Big[\underbrace{\mathbb{E}_{q_1^\omega \sim p(\cdot|x,\omega)}\mathbb{E}_{q_2^{\omega^*} \sim p(\cdot|x,\omega^*)}\left[s(q_1^\omega, q_2^{\omega^*})\right]}_{\text{cross-model similarity}} - \underbrace{\mathbb{E}_{r_1^\omega \sim p(\cdot|x,\omega)}\mathbb{E}_{r_2^\omega \sim p(\cdot|x,\omega)}\left[s(r_1^\omega, r_2^\omega)\right]}_{\text{self-similarity (1 - AU)}}\Big]. \tag{2}$$

In effect, $D(\omega \,||\, \omega^*)$ measures the difference between 1) the similarity of responses from ω and ω^* $\left(\mathbb{E}_{q_1^\omega \sim p(\cdot|x,\omega)}\mathbb{E}_{q_2^{\omega^*} \sim p(\cdot|x,\omega^*)}\left[s(q_1^\omega, q_2^{\omega^*})\right]\right)$ and 2) the self-similarity of ω $\left(\mathbb{E}_{r_1^\omega \sim p(\cdot|x,\omega)}\mathbb{E}_{r_2^\omega \sim p(\cdot|x,\omega)}\left[s(r_1^\omega, r_2^\omega)\right]\right)$. In the case where ω is optimal and equivalent to ω^*, then $D(\omega \,||\, \omega^*)$ will be 0. When ω produces responses that are semantically diverse from the ideal model's responses even after accounting for the diversity due to ω's aleatoric uncertainty, then $D(\omega \,||\, \omega^*)$ will be high. In practice, we do not have access to the optimal model ω^*. Instead, we can leverage a recent information-theoretic technique (Schweighofer et al., 2023) and marginalize out ω^*. Let P_Ω be a distribution over models such that $\mathbb{E}_{\tilde{\omega} \sim P_\Omega}\left[p(\cdot \mid x; \tilde{\omega})\right] = p(\cdot \mid x)$. We can thus replace ω^* in Equation 2 with an expectation over P_Ω, and define $U_{\text{epistemic}}(x, \omega)$ as:

$$\begin{aligned} U_{\text{epistemic}}(x, \omega) = &- \mathbb{E}_{\tilde{\omega} \sim P_\Omega}\left[\mathbb{E}_{q_1^\omega \sim p(\cdot|x,\omega)}\mathbb{E}_{q_2^{\tilde{\omega}} \sim p(\cdot|x,\tilde{\omega})}\left[s(q_1^\omega, q_2^{\tilde{\omega}})\right]\right] \\ &+ \mathbb{E}_{r_1^\omega \sim p(\cdot|x,\omega)}\mathbb{E}_{r_2^\omega \sim p(\cdot|x,\omega)}\left[s(r_1^\omega, r_2^\omega)\right]. \end{aligned} \tag{3}$$

When the average similarity in responses between ω and other sampled models matches the self-similarity of ω's responses, then the semantic distribution of ω matches the target distribution and the epistemic uncertainty is low. When there is a mismatch between the average similarity of ω's responses to the responses from the sampled models $\tilde{\omega}$ compared to ω's self-similarity, then there is a disagreement in how models respond and the epistemic uncertainty is high. In Appendix A.1, we provide a detailed interpretation of $D(\omega \,\|\, \omega^*)$ as a one-sided kernel discrepancy, establish its connections to variational inference, and show that it is upper bounded by total variation distance under mild conditions.

Desired Properties for Ω. Because the divergence $D(\omega \,||\, \omega^*)$ is evaluated against samples drawn from a *surrogate* distribution of models Ω, its fidelity hinges on how well that ensemble of models approximates the (inaccessible) optimal distribution $p(\cdot \mid x; \omega^*)$. Three criteria follow from the definition in Eq. 3:

(i) **Support richness.** Ω covers distinct yet plausible interpretations of models, rather than a narrow subset; otherwise the cross–similarity term in D may be artificially high, and D underestimates EU when predictions of models in Ω are different from ω's predictions.

(ii) **Non-collapsing diversity.** If all members of Ω are nearly identical (e.g. noise-perturbed versions of the same model), the ensemble average would be too close to ω, hence the cross-model similarity term will be close to self-similarity and D may be small, even when the candidate predictor P_ω is *mis-specified*.

(iii) **Calibrated weighting.** Let P_Ω denote the mixing measure over models. For Eq. 3 to approach the ideal $p(y \mid x)$, each model should be weighted in proportion to its posterior credibility (e.g. uniform weights are appropriate only when validation risks are comparable).

Achieving Properties via Cross-Family Models. A practical way to satisfy these criteria is to construct the surrogate ensemble Ω from models of similar architecture and scale, likely trained on overlapping or similar pre-training datasets. Specifically, we populate Ω with 7–9B Transformer-based models that share the *same architecture class* but are trained by *different vendors*. This setup ensures (i) *support richness*, as models differ in data pipelines, initializations, and alignment protocols, which results in diverse but plausible responses for the same input, that cover the ground-truth response set. These independently trained models also exhibit (ii) *non-collapsing diversity*, as their differences arise from different design choices, rather than noise-perturbed versions of a single model. Finally, because these models achieve similar validation performance, we adopt uniform weights in P_Ω, which satisfies the *calibrated weighting* (iii) requirement. Section 4 specifies the exact models used.

Total Predictive Uncertainty. We make the standard assumption that total predictive uncertainty can be obtained by adding aleatoric and epistemic predictive uncertainties (Hüllermeier & Waegeman,

2021). Thus, we define $U_{\text{total}}(x;\omega)$ as:

$$\begin{aligned} U_{\text{total}}(x;\omega) &= U_{\text{aleatoric}}(x;\omega) + U_{\text{epistemic}}(x;\omega) \\ &= \mathbb{E}_{\tilde{\omega}\sim P_\Omega}\mathbb{E}_{r_1^\omega \sim p(\cdot|x,\omega)}\mathbb{E}_{q_2^{\tilde{\omega}} \sim p(\cdot|x,\tilde{\omega})}\big[1 - s(r_1^\omega, q_2^{\tilde{\omega}})\big]. \end{aligned} \tag{4}$$

3.3 Empirical Estimates of Uncertainty Metrics

For a given input prompt x, we call the model whose uncertainty is being estimated the *reference model* ω, and denote the set of models used to compute epistemic uncertainty with respect to the reference as the *auxiliary model set* Ω. Throughout the paper, we mainly focus on *Cross-family auxiliary models*: We estimate epistemic uncertainty by computing response divergence across an auxiliary set of models. To estimate uncertainty in practice, we proceed as follows:

1. Sample n responses from each model $\omega_i \in \Omega$, and denote the set of responses from ω as $R' = \{r'_1, r'_2, \ldots, r'_n\}$ and from ω_i as $R_i = \{r_1^{(i)}, r_2^{(i)}, \ldots, r_n^{(i)}\}$ where $|\Omega| = m$.
2. Approximate Aleatoric, Total, and Epistemic Uncertainty using these sampled responses.

Empirical Uncertainty Metrics

$$AU = U_{\text{aleatoric}} = 1 - \big[\sum_{k=1}^{n}\sum_{j=1}^{n} s(r'_k, r'_j)\big]/n^2$$

$$TU = U_{\text{total}} = 1 - \frac{1}{m}\sum_{i=1}^{m}\big[\sum_{k=1}^{n}\sum_{j=1}^{n} s(r'_k, r_j^{(i)})\big]/n^2$$

$$EU = U_{\text{epistemic}} = U_{\text{total}} - U_{\text{aleatoric}}$$

Note that we assign uniform weights to different models in the auxiliary set, as we choose to use models of similar capabilities, and our estimate of AU is similar to the one from Lin et al. (2023). Also, observe that our evaluation shows that we can keep the overall number of sampled responses at the magnitude used by self-consistency based methods while improving over those. More concretely, we choose $n = \frac{n'}{m}$, when comparing to AU as a standalone metric, where n' is the number of samples used for the latter.

4 Experimental Setup

Models. In the main experiments, we primarily focus on five instruction-tuned language models with approximately 7–9B parameters: `Gemma-2-9B-It` (Team et al., 2024), `Granite-3.0-8B-Instruct` (Granite Team, 2024), `Llama-3.1-8B-Instruct` (Grattafiori et al., 2024), `Mistral-7B-Instruct-v0.3` (Jiang et al., 2023),

`Qwen2.5-7B-Instruct` (Yang et al., 2024). We compute the uncertainty measures from Section 3.3 and consider the models mentioned above as the set of auxiliary models. In Appendix A.5, we also consider larger reference models. Unless otherwise noted, we compute TU by sampling 2 responses from each of the 5 models and similarly compute AU using 10 samples to keep the sampling budget the same across the two metrics.

Datasets. Our experiments cover a broad range of long-form generation tasks spanning question answering (QA), math reasoning, translation, and summarization. For QA, we include `AmbigQA` (Min et al., 2020) (open-domain QA with both ambiguous and unambiguous questions), `NQ-open` (Kwiatkowski et al., 2019) (closed-book QA derived from real user queries), `HotpotQA` (Yang et al., 2018) (multi-hop QA requiring reasoning over multiple supporting documents), `CoQA` (Reddy et al., 2019) (conversational QA with multiple turns), `QASPER` (Dasigi et al., 2021) (fact-based QA over long scientific papers), `TriviaQA` (Joshi et al., 2017) (QA based on trivia-style questions), and `TruthfulQA` (Lin et al., 2021) (QA to evaluate common misconceptions in models). For math reasoning, we use `GSM8K` (Cobbe et al., 2021) with chain-of-thought prompting. For language generation, we evaluate on the German-to-English translation dataset `WMT16-de-en` (Bojar et al., 2016) and the summarization benchmark `XSum` (Narayan et al., 2018).

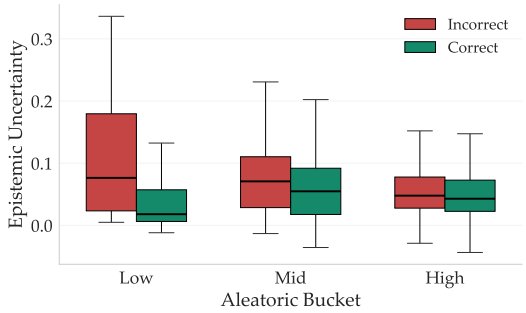

(a) We stratify examples by AU (low, mid, high; 33% each) and compare the distribution of EU for correct and incorrect generations. Incorrect responses show higher EU in the low-AU regime, but this separation weakens as AU increases.

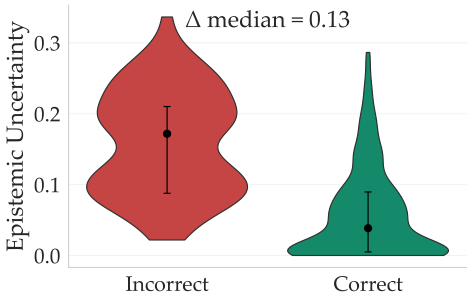

(b) We isolate the most confident samples (lowest 5% AU) and find that incorrect generations have significantly higher EU than correct ones, which shows that EU effectively flags confidently wrong predictions.

Figure 2: Based on the distribution of EU across samples with different AU values, we find that EU separates incorrect from correct most strongly when AU is low.

We additionally include `SimpleQA` (Wei et al., 2024), a factuality QA benchmark, with model responses generated by `GPT-4o` (Hurst et al., 2024) and `Claude 3.7 Sonnet` (Claude). Finally, we adapt tasks from the BBH multiple-choice benchmark (Suzgun et al., 2022) to long-form format and add those evaluations to Appendix A.7.

Evaluation. Correctness is defined per input-response pair using `Meta-Llama-3-70B-Instruct` as judge (Appendix A.10). Note that, in the context of uncertainty estimation, LM-as-a-judge correctness evaluation has recently been shown to be the most reliable among the existing methods (Santilli et al., 2025). Following prior work (Lin et al., 2023; Kuhn et al., 2023a; Band et al., 2022), we evaluate the quality of uncertainty by quantifying how well uncertainty scores separate correct from incorrect generations, using Area Under the ROC Curve (AUROC). Formally, AUROC corresponds to the probability that a randomly chosen incorrect response receives a higher uncertainty score than a randomly chosen correct one.

We also evaluate effectiveness in terms of selective prediction using Risk–Coverage Curves (Nadeem et al., 2009), which measures how the error rate changes as uncertain responses are rejected. We further report standard summary metrics such as accuracy at 90% and 80% coverage (C@90 and C@80), and the Area Under Risk-Coverage Curve (AURC), where lower is better.

Baselines. As our primary aleatoric baseline, we use Lin et al. (2023)'s implementation of Aleatoric Uncertainty, which is in practice similar to Semantic Entropy (Kuhn et al., 2023a), and has been shown to perform well in recent benchmarks and surveys (Fadeeva et al., 2023; Vashurin et al., 2025). In our evaluation, we denote this baseline as Aleatoric or AU. We also experiment with noise-perturbed models (i.e., instead of models from different model families), similar to the approach of Liu et al. (2025), see details in Appendix A.5.

5 Results

5.1 Epistemic Uncertainty Flags Confident Failures of Aleatoric Uncertainty

Language models are often applied to heterogeneous tasks, where model confidence does not always align with correctness (Zhou et al., 2024). To simulate such a setting, we construct an aggregated dataset by combining all datasets mentioned in Section 4, and analyze uncertainty trends on this pooled distribution. We are particularly interested in identifying failure modes of AU.

In Figure 2a, we stratify examples by AU (low, mid, high) and compare EU across correct and incorrect responses. In the low-AU regime, incorrect responses exhibit higher EU than correct ones, which shows that EU is discriminative when aleatoric scores are overconfident. This separation diminishes in higher AU buckets, where both response groups become more uncertain. To more directly target this failure mode, we isolate the lowest 5% of AU scores and analyze EU by correctness. (Figure 2b). EU remains significantly higher for incorrect generations, which confirms that epistemic

uncertainty flags confidently wrong outputs that aleatoric scores alone miss, which supports our hypothesis of the complementary nature of scores in this particular AU region.

This result contrasts with prior work, which treats low-AU predictions as reliable and only incorporates cross-model comparisons when AU exceeds a threshold (Xue et al., 2025; Chen et al., 2025). Our findings reveal that this assumption overlooks a critical failure mode: confidently wrong predictions with low AU. On the other hand, our observations validate findings about models being overconfident on `HotpotQA` (Ni et al., 2024) in that incorporating EU yields large improvements on this dataset (see Figure 4 in Section 5.3). Per-dataset results are provided in Figure 18 in Appendix A.8.

5.2 Epistemic Uncertainty, Agreement, and Diversity

We ask *when* similarity-based EU is most informative. To this end, we focus on the correctness of responses of different models and consider two metrics: *Jaccard Agreement* (or *Redundancy*) (J), which measures the overlap between predicted correct responses of the auxiliary models, used to quantify how redundant or similar different predictions are; and *Oracle Coverage Gain* (also *Complementarity*) (G), the additional coverage (i.e., improvement in accuracy) obtained by an oracle that always chooses the correct model per example, over the best performing model. Exact definitions can be found in Appendix A.2.

Epistemic uncertainty does not always coincide with inter-model disagreement. Figure 3 plots EU AUROC against the dataset-level statistics J and G. We observe a positive correlation with redundancy ($r = +0.72,\ p = 0.03$) and a negative correlation with complementarity ($r = -0.72,\ p = 0.03$), which is the opposite of the naive intuition that "more disagreement $\Rightarrow$ higher epistemic utility."

The explanation lies in how EU is constructed: it grows with the *divergence of generated answers*, which arises in two distinct cases: (i) true EU on intrinsically hard questions where models do not know the answer, and (ii) the existence of many semantically different but correct responses (response noise). In complementary datasets (large G), each model specializes on different niches and consequently, EU is large even on questions that an individual model answers correctly, because models in the auxiliary set return alternative (wrong) responses. In such cases, the misalignment with correctness drives AUROC down. Conversely, in redundant datasets (high J, low G), models converge to similar responses when correct (EU low) and, what we expect to be the usual case, still diverge when collectively wrong (EU high), which gives a well-separated score and high AUROC. These observations characterize the cases in which our current EU estimator is effective: tasks with a single (or near-unique) correct answer, where models phrase that answer similarly yet generate diverse alternatives on the harder, unanswered inputs.

For example, `WMT16-de-en` and `CoQA` occupy the high-J, low-G corner of Figure 3; all models score above $> 90\%$ accuracy, so predictions are largely redundant and EU achieves its strongest

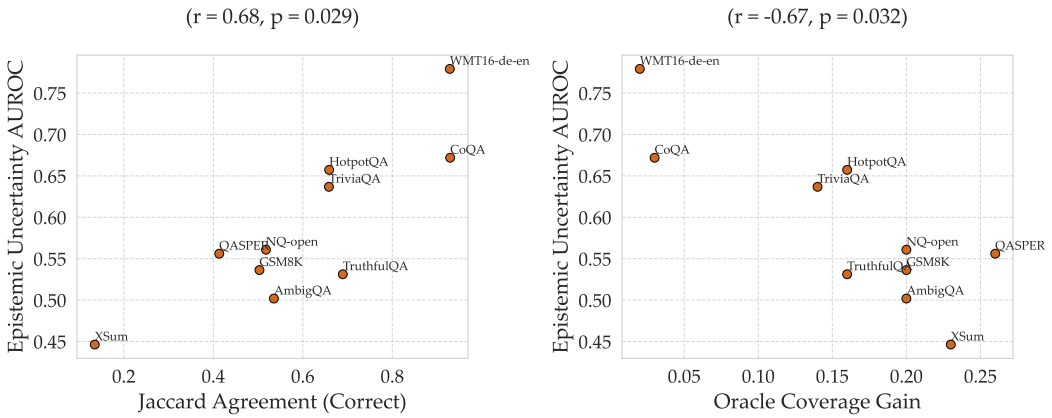

Figure 3: Epistemic uncertainty AUROC versus dataset level redundancy (J) and complementarity (G). Higher AUROC indicates better discrimination between correct and incorrect answers by EU.

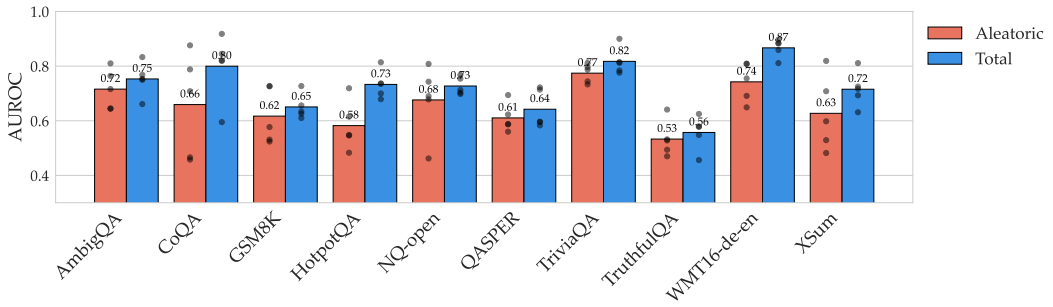

Figure 4: Under matched sample budgets, TU (AU+EU) consistently shows higher AUROC than AU across datasets, with the largest gains on `HotpotQA`, `CoQA`, and `WMT16-de-en` (Δ >0.10). Bars show means over five 7–9B reference models with per-dataset dots.

discrimination. At the opposite extreme, `XSum` combines low accuracy with the largest G: models succeed on different inputs and can express many valid summaries, which inflates EU without improving ranking and thus lowering AUROC. Datasets such as `HotpotQA` and `TriviaQA` sit mid-range on both axes and have enough redundancy to suppress noise, but have sufficient diversity to expose disagreement and consequently produce the large TU gains in Figure 4.

5.3 Total Uncertainty Improves Correctness Calibration

Figure 4 reports the AUROC between negative uncertainty and correctness across datasets, and averaged over five 7–9B instruction-tuned models mentioned in Section 4. TU consistently improves over AU on all benchmarks on average. The largest gains occur on `HotpotQA` (+0.15), `CoQA` (+0.14), and `WMT16-de-en` (+0.13), where models either disagree on complex multi-hop reasoning (`HotpotQA`) or achieve high overall accuracy (`CoQA`, `WMT16-de-en`), which allows EU to capture remaining errors.

Moderate improvements are observed on `TriviaQA`, and `NQ-open`, which exhibit a balance of response *redundancy* and *complementarity*. In contrast, gains are more limited on `TruthfulQA`, `GSM8K` (with chain-of-thought), and `QASPER`, where the presence of multiple valid or stylistically diverse answers weakens the alignment between TU and correctness. These results align with the patterns described in Section 5.2: TU and EU are most effective when correct answers are uniquely phrased and shared across models, while incorrect predictions remain diverse.

We also find that TU estimates consistently improve AUROC as compared to AU in `GPT-4o` (0.70 vs. 0.59), and `Claude 3.7 Sonnet` (0.58 vs. 0.53) on `SimpleQA` as shown in Figure 1. Figure 11 in Appendix A.4 shows the ROC curves on the combination of all datasets, where the relative ranking

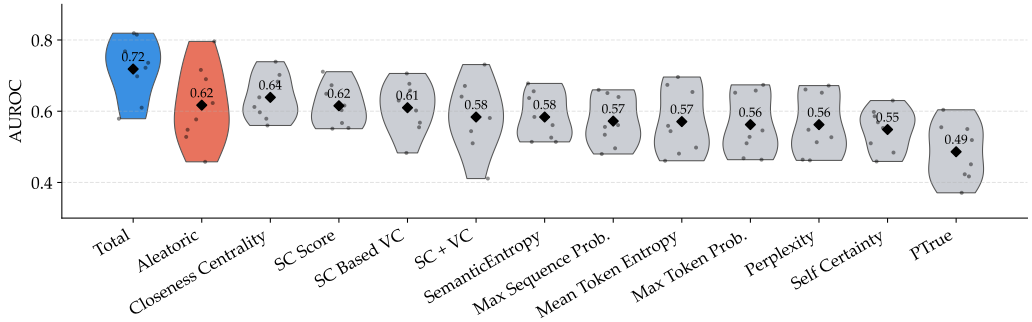

Figure 5: Using `Mistral-7B-Instruct-v0.3` as the reference model, TU attains the best mean AUROC (0.72), and outperforms the strongest baseline (closeness centrality, 0.64) across almost all datasets. Per-task results appear in Table 3 in Appendix A.4.

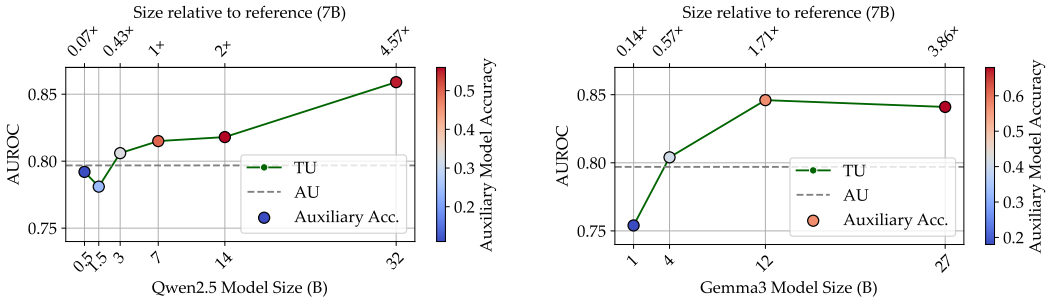

Figure 6: We keep the reference model fixed as `mistral-7B`, and vary the size of the **single auxiliary model**. TU achieves higher AUROC in comparison to AU, even in cases where the size of the auxiliary model is lower than ($\times 0.43$) or roughly the same ($\times 1$) as the reference model. The improvements are more significant with larger and more capable the auxiliary models on `TriviaQA`.

of data points across the whole dataset determines performance, and Table 2 reports AUROC per model-dataset pair. We show that the improvement over AU is maintained in individual datasets, and in the combination of all datasets.

Comparison to Baselines. We compare TU against a number of baselines: Mean Token Entropy (Fomicheva et al., 2020), Maximum Token Probability (Fadeeva et al., 2023), Maximum Sequence Probability (Fadeeva et al., 2023), Perplexity (Fomicheva et al., 2020), PTrue (Kadavath et al., 2022), Self-Certainty (Kang et al., 2025), Semantic Entropy (Kuhn et al., 2023a), SC (Self-Consistency) Score (Wang et al., 2022; Manakul et al., 2023), Closeness Centrality, SC + VC (Verbalized confidence), and SC based CV (Jiang et al., 2024). Figure 5 shows results for `Mistral-7B-Instruct-v0.3` as the reference model across benchmarks and baselines. Table 3 in Appendix A.4 shows that TU outperforms the strongest baseline across almost all benchmarks.

Ablations. We further ablate the size of the reference model in Appendix A.5, and show that even in scenarios where the reference model is larger (and has higher accuracy) than models in the auxiliary set, TU still achieves higher AUROC than AU. Furthermore, we show that AUROC improves with a larger number of sampled responses in Appendix A.6.

5.4 Total Uncertainty Improves Selective Abstention

To evaluate whether uncertainty effectively distinguishes reliable responses from potential errors, we consider selective prediction, where models are allowed to abstain from answering when uncertain.

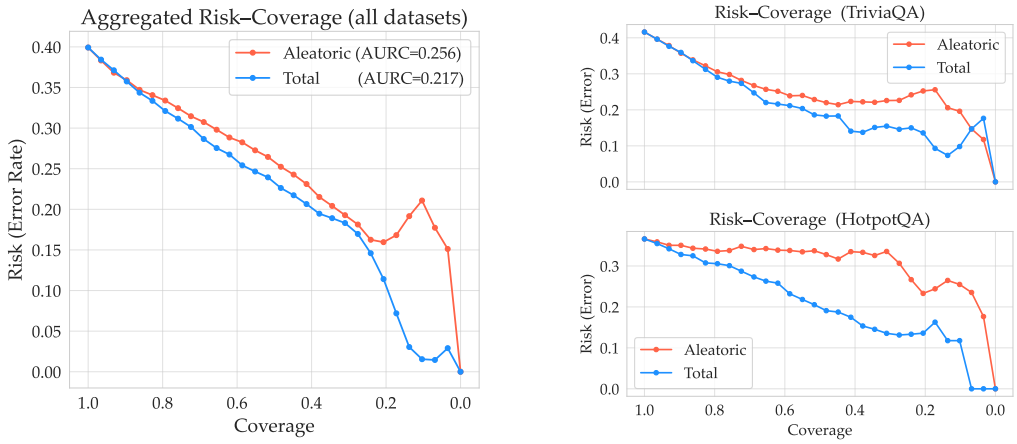

Figure 7: Risk–coverage analysis shows that TU consistently improves selective prediction across datasets and in aggregate.

Risk-Coverage Tradeoff. Figure 7(a) shows the Risk-coverage curve for aleatoric and total uncertainty, aggregated across all models mentioned in Section 4. Across all coverage levels and datasets, total uncertainty achieves the lowest risk, with a single exception. This suggests that total uncertainty more effectively identifies unreliable predictions in comparison to AU.

Selective Accuracy and AURC. To quantify this effect more precisely, Table 1 reports selective accuracy at fixed coverage levels (C@90, C@80) and AURC (area under the risk–coverage curve) across benchmarks and averaged over different models. In nearly all cases, total uncertainty achieves higher selective accuracy and in all cases lower AURC compared to aleatoric and EU alone. For example, on `HotpotQA` and `XSum`, total uncertainty improves C@90 by over 1.5 points and reduces area under the risk–coverage curve (AURC ↓) by over 20%. These results confirm that TU yields better abstention behavior than AU or EU alone.

Table 1: Selective question answering performance of different uncertainty estimates.

Dataset	C@90 (%)			C@80 (%)			AURC ↓		
	Aleatoric	Epistemic	Total	Aleatoric	Epistemic	Total	Aleatoric	Epistemic	Total
`AmbigQA`	56.0	52.4	**56.2**	59.5	53.2	**60.2**	0.325	0.456	**0.278**
`CoQA`	96.0	**96.9**	96.0	96.5	97.5	**97.8**	0.026	0.016	**0.011**
`GSM8K`	54.0	**54.7**	53.3	**54.8**	54.0	54.2	0.391	0.441	**0.335**
`HotpotQA`	64.9	66.2	**66.9**	66.2	67.2	**69.2**	0.304	0.257	**0.206**
`NQ-open`	**53.8**	51.3	53.1	57.2	52.8	**57.5**	0.388	0.484	**0.323**
`QASPER`	38.0	36.9	**39.1**	39.5	37.5	**40.8**	0.533	0.602	**0.503**
`TriviaQA`	**64.0**	60.4	**64.0**	69.0	61.8	**70.2**	0.254	0.343	**0.208**
`TruthfulQA`	**74.4**	73.8	74.2	**75.0**	**75.0**	73.0	0.220	0.251	**0.195**
`WMT16-de-en`	96.2	**96.4**	96.0	97.2	96.2	**98.5**	0.028	0.027	**0.010**
`XSum`	24.4	24.9	**25.6**	26.5	22.0	**27.3**	0.681	0.759	**0.609**

6 Conclusions

We propose that aleatoric and epistemic uncertainty capture complementary failure modes of language models: self-consistency methods reveal data ambiguity, while semantic disagreement across models uncovers uncertainty arising from model limitations. We operationalize this view by estimating TU as the combination of intra-model entropy and inter-model semantic divergence, using only black-box access to model outputs. We show that this combination effectively outperforms self-consistency-based methods across a wide range of models and datasets in terms of different metrics. While this approach requires access to multiple comparable models, it reveals the limits of single-model uncertainty scores and offers a practical path toward more comprehensive uncertainty estimation.

Limitations. Our method relies on response-level semantic similarity, which may underperform in tasks with many semantically distinct but correct answers, e.g., open-ended generation or QA tasks where there are multiple distinct correct answers. In such cases, disagreement does not necessarily reflect uncertainty. Additionally, we focus on a specific form of AU; how to best combine our EU estimator with other AU and EU estimators (e.g., token-level or logit-based methods) is left for future work. Moreover, the performance of TU depends on the model ensemble: If all surrogate models share similar pre-training data or architectural biases, cross-model disagreement can underestimate true epistemic uncertainty. We examine this homogeneous-failure scenario in detail in Section 5.2. Finally, our evaluation hinges on a correctness judge; improvements in judge reliability will propagate to more precise AUROC and selective-risk estimates.

REFERENCES

Yasin Abbasi Yadkori, Ilja Kuzborskij, András György, and Csaba Szepesvari. To believe or not to believe your llm: Iterative prompting for estimating epistemic uncertainty. *Advances in Neural Information Processing Systems*, 37:58077–58117, 2024.

Lukas Aichberger, Kajetan Schweighofer, Mykyta Ielanskyi, and Sepp Hochreiter. Semantically diverse language generation for uncertainty estimation in language models. *arXiv preprint arXiv:2406.04306*, 2024.

Neil Band, Tim GJ Rudner, Qixuan Feng, Angelos Filos, Zachary Nado, Michael W Dusenberry, Ghassen Jerfel, Dustin Tran, and Yarin Gal. Benchmarking bayesian deep learning on diabetic retinopathy detection tasks. *arXiv preprint arXiv:2211.12717*, 2022.

Ondrej Bojar, Rajen Chatterjee, Christian Federmann, Yvette Graham, Barry Haddow, Matthias Huck, Antonio Jimeno Yepes, Philipp Koehn, Varvara Logacheva, Christof Monz, et al. Findings of the 2016 conference on machine translation (wmt16). In *First conference on machine translation*, pp. 131–198. Association for Computational Linguistics, 2016.

Tapabrata Chakraborti, Christopher RS Banerji, Ariane Marandon, Vicky Hellon, Robin Mitra, Brieuc Lehmann, Leandra Bräuninger, Sarah McGough, Cagatay Turkay, Alejandro F Frangi, et al. Personalized uncertainty quantification in artificial intelligence. *Nature Machine Intelligence*, 7(4): 522–530, 2025.

Jianhao Chen, Zishuo Xun, Bocheng Zhou, Han Qi, Qiaosheng Zhang, Yang Chen, Wei Hu, Yuzhong Qu, Wanli Ouyang, and Shuyue Hu. Do we truly need so many samples? multi-llm repeated sampling efficiently scale test-time compute. *arXiv preprint arXiv:2504.00762*, 2025.

Claude. Claude 3.7 sonnet system card. URL https://api.semanticscholar.org/CorpusID:276612236.

Karl Cobbe, Vineet Kosaraju, Mohammad Bavarian, Mark Chen, Heewoo Jun, Lukasz Kaiser, Matthias Plappert, Jerry Tworek, Jacob Hilton, Reiichiro Nakano, et al. Training verifiers to solve math word problems. *arXiv preprint arXiv:2110.14168*, 2021.

Ben Cottier, Robi Rahman, Loredana Fattorini, Nestor Maslej, Tamay Besiroglu, and David Owen. The rising costs of training frontier ai models. *arXiv preprint arXiv:2405.21015*, 2024.

Pradeep Dasigi, Kyle Lo, Iz Beltagy, Arman Cohan, Noah A Smith, and Matt Gardner. A dataset of information-seeking questions and answers anchored in research papers. *arXiv preprint arXiv:2105.03011*, 2021.

Prasenjit Dey, Srujana Merugu, and Sivaramakrishnan Kaveri. Uncertainty-aware fusion: An ensemble framework for mitigating hallucinations in large language models. *arXiv preprint arXiv:2503.05757*, 2025.

Ekaterina Fadeeva, Roman Vashurin, Akim Tsvigun, Artem Vazhentsev, Sergey Petrakov, Kirill Fedyanin, Daniil Vasilev, Elizaveta Goncharova, Alexander Panchenko, Maxim Panov, et al. Lm-polygraph: Uncertainty estimation for language models. *arXiv preprint arXiv:2311.07383*, 2023.

Marina Fomicheva, Shuo Sun, Lisa Yankovskaya, Frédéric Blain, Francisco Guzmán, Mark Fishel, Nikolaos Aletras, Vishrav Chaudhary, and Lucia Specia. Unsupervised quality estimation for neural machine translation. *Transactions of the Association for Computational Linguistics*, 8: 539–555, 2020.

Yarin Gal and Zoubin Ghahramani. Dropout as a bayesian approximation: Representing model uncertainty in deep learning. In *international conference on machine learning*, pp. 1050–1059. PMLR, 2016.

Shiqi Gao, Tianxiang Gong, Zijie Lin, Runhua Xu, Haoyi Zhou, and Jianxin Li. Flue: Streamlined uncertainty estimation for large language models. In *Proceedings of the AAAI Conference on Artificial Intelligence*, volume 39, pp. 16745–16753, 2025.

Xiang Gao, Jiaxin Zhang, Lalla Mouatadid, and Kamalika Das. Spuq: Perturbation-based uncertainty quantification for large language models. *arXiv preprint arXiv:2403.02509*, 2024.

IBM Granite Team. Granite 3.0 language models, October 2024. URL https://github.com/ibm-granite/granite-3.0-language-models/.

Aaron Grattafiori, Abhimanyu Dubey, Abhinav Jauhri, Abhinav Pandey, Abhishek Kadian, Ahmad Al-Dahle, Aiesha Letman, Akhil Mathur, Alan Schelten, Alex Vaughan, et al. The llama 3 herd of models. *arXiv preprint arXiv:2407.21783*, 2024.

HW Chung L Hou, S Longpre, B Zoph, Y Tay, W Fedus, Y Li, X Wang, M Dehghani, S Brahma, and A Webson. Scaling instruction-finetuned language models. *arXiv preprint arXiv:2210.11416*, 2022.

Eyke Hüllermeier and Willem Waegeman. Aleatoric and epistemic uncertainty in machine learning: An introduction to concepts and methods. *Machine learning*, 110(3):457–506, 2021.

Aaron Hurst, Adam Lerer, Adam P Goucher, Adam Perelman, Aditya Ramesh, Aidan Clark, AJ Ostrow, Akila Welihinda, Alan Hayes, Alec Radford, et al. Gpt-4o system card. *arXiv preprint arXiv:2410.21276*, 2024.

Mykyta Ielanskyi, Kajetan Schweighofer, Lukas Aichberger, and Sepp Hochreiter. Addressing pitfalls in the evaluation of uncertainty estimation methods for natural language generation. In *ICLR Workshop: Quantify Uncertainty and Hallucination in Foundation Models: The Next Frontier in Reliable AI*.

Albert Q Jiang, A Sablayrolles, A Mensch, C Bamford, D Singh Chaplot, Ddl Casas, F Bressand, G Lengyel, G Lample, L Saulnier, et al. Mistral 7b. arxiv. *arXiv preprint arXiv:2310.06825*, 10, 2023.

Mingjian Jiang, Yangjun Ruan, Prasanna Sattigeri, Salim Roukos, and Tatsunori B Hashimoto. Graph-based uncertainty metrics for long-form language model generations. *Advances in Neural Information Processing Systems*, 37:32980–33006, 2024.

Daniel D Johnson, Daniel Tarlow, David Duvenaud, and Chris J Maddison. Experts don't cheat: learning what you don't know by predicting pairs. *arXiv preprint arXiv:2402.08733*, 2024.

Mandar Joshi, Eunsol Choi, Daniel S Weld, and Luke Zettlemoyer. Triviaqa: A large scale distantly supervised challenge dataset for reading comprehension. *arXiv preprint arXiv:1705.03551*, 2017.

Saurav Kadavath, Tom Conerly, Amanda Askell, Tom Henighan, Dawn Drain, Ethan Perez, Nicholas Schiefer, Zac Hatfield-Dodds, Nova DasSarma, Eli Tran-Johnson, et al. Language models (mostly) know what they know. *arXiv preprint arXiv:2207.05221*, 2022.

Zhewei Kang, Xuandong Zhao, and Dawn Song. Scalable best-of-n selection for large language models via self-certainty. *arXiv preprint arXiv:2502.18581*, 2025.

Andreas Kirsch. (implicit) ensembles of ensembles: Epistemic uncertainty collapse in large models. *arXiv preprint arXiv:2409.02628*, 2024.

Jannik Kossen, Jiatong Han, Muhammed Razzak, Lisa Schut, Shreshth Malik, and Yarin Gal. Semantic entropy probes: Robust and cheap hallucination detection in llms. *arXiv preprint arXiv:2406.15927*, 2024.

Lorenz Kuhn, Yarin Gal, and Sebastian Farquhar. Semantic uncertainty: Linguistic invariances for uncertainty estimation in natural language generation. *arXiv preprint arXiv:2302.09664*, 2023a.

Lorenz Kuhn, Yarin Gal, and Sebastian Farquhar. Semantic uncertainty: Linguistic invariances for uncertainty estimation in natural language generation. In *ICLR*, 2023b.

Tom Kwiatkowski, Jennimaria Palomaki, Olivia Redfield, Michael Collins, Ankur Parikh, Chris Alberti, Danielle Epstein, Illia Polosukhin, Jacob Devlin, Kenton Lee, et al. Natural questions: a benchmark for question answering research. *Transactions of the Association for Computational Linguistics*, 7:453–466, 2019.

Woosuk Kwon, Zhuohan Li, Siyuan Zhuang, Ying Sheng, Lianmin Zheng, Cody Hao Yu, Joseph E. Gonzalez, Hao Zhang, and Ion Stoica. Efficient memory management for large language model serving with pagedattention. In *Proceedings of the ACM SIGOPS 29th Symposium on Operating Systems Principles*, 2023.

Balaji Lakshminarayanan, Alexander Pritzel, and Charles Blundell. Simple and scalable predictive uncertainty estimation using deep ensembles. *Advances in neural information processing systems*, 30, 2017.

Shalev Lifshitz, Sheila A McIlraith, and Yilun Du. Multi-agent verification: Scaling test-time compute with multiple verifiers. *arXiv preprint arXiv:2502.20379*, 2025.

Stephanie Lin, Jacob Hilton, and Owain Evans. Truthfulqa: Measuring how models mimic human falsehoods. *arXiv preprint arXiv:2109.07958*, 2021.

Stephanie Lin, Jacob Hilton, and Owain Evans. Teaching models to express their uncertainty in words. *arXiv preprint arXiv:2205.14334*, 2022.

Zhen Lin, Shubhendu Trivedi, and Jimeng Sun. Generating with confidence: Uncertainty quantification for black-box large language models. *arXiv preprint arXiv:2305.19187*, 2023.

Linyu Liu, Yu Pan, Xiaocheng Li, and Guanting Chen. Uncertainty estimation and quantification for llms: A simple supervised approach. *arXiv preprint arXiv:2404.15993*, 2024.

Litian Liu, Reza Pourreza, Sunny Panchal, Apratim Bhattacharyya, Yao Qin, and Roland Memisevic. Enhancing hallucination detection through noise injection. *arXiv preprint arXiv:2502.03799*, 2025.

Jinliang Lu, Ziliang Pang, Min Xiao, Yaochen Zhu, Rui Xia, and Jiajun Zhang. Merge, ensemble, and cooperate! a survey on collaborative strategies in the era of large language models. *arXiv preprint arXiv:2407.06089*, 2024.

Huan Ma, Jingdong Chen, Guangyu Wang, and Changqing Zhang. Estimating llm uncertainty with logits. *arXiv preprint arXiv:2502.00290*, 2025.

Potsawee Manakul, Adian Liusie, and Mark JF Gales. Selfcheckgpt: Zero-resource black-box hallucination detection for generative large language models. *arXiv preprint arXiv:2303.08896*, 2023.

Sewon Min, Julian Michael, Hannaneh Hajishirzi, and Luke Zettlemoyer. Ambigqa: Answering ambiguous open-domain questions. *arXiv preprint arXiv:2004.10645*, 2020.

Malik Sajjad Ahmed Nadeem, Jean-Daniel Zucker, and Blaise Hanczar. Accuracy-rejection curves (arcs) for comparing classification methods with a reject option. In *Machine Learning in Systems Biology*, pp. 65–81. PMLR, 2009.

Shashi Narayan, Shay B Cohen, and Mirella Lapata. Don't give me the details, just the summary! topic-aware convolutional neural networks for extreme summarization. *arXiv preprint arXiv:1808.08745*, 2018.

Jianmo Ni, Gustavo Hernandez Abrego, Noah Constant, Ji Ma, Keith B Hall, Daniel Cer, and Yinfei Yang. Sentence-t5: Scalable sentence encoders from pre-trained text-to-text models. *arXiv preprint arXiv:2108.08877*, 2021.

Shiyu Ni, Keping Bi, Jiafeng Guo, and Xueqi Cheng. When do llms need retrieval augmentation? mitigating llms' overconfidence helps retrieval augmentation. *arXiv preprint arXiv:2402.11457*, 2024.

Alexander Nikitin, Jannik Kossen, Yarin Gal, and Pekka Marttinen. Kernel language entropy: Fine-grained uncertainty quantification for llms from semantic similarities. *Advances in Neural Information Processing Systems*, 37:8901–8929, 2024.

Siva Reddy, Danqi Chen, and Christopher D Manning. Coqa: A conversational question answering challenge. *Transactions of the Association for Computational Linguistics*, 7:249–266, 2019.

Andrea Santilli, Adam Golinski, Michael Kirchhof, Federico Danieli, Arno Blaas, Miao Xiong, Luca Zappella, and Sinead Williamson. Revisiting uncertainty quantification evaluation in language models: Spurious interactions with response length bias results. *arXiv preprint arXiv:2504.13677*, 2025.

Kajetan Schweighofer, Lukas Aichberger, Mykyta Ielanskyi, and Sepp Hochreiter. Introducing an improved information-theoretic measure of predictive uncertainty. *arXiv preprint arXiv:2311.08309*, 2023.

Tal Shnitzer, Anthony Ou, Mírian Silva, Kate Soule, Yuekai Sun, Justin Solomon, Neil Thompson, and Mikhail Yurochkin. Large language model routing with benchmark datasets. *arXiv preprint arXiv:2309.15789*, 2023.

Ola Shorinwa, Zhiting Mei, Justin Lidard, Allen Z Ren, and Anirudha Majumdar. A survey on uncertainty quantification of large language models: Taxonomy, open research challenges, and future directions. *arXiv preprint arXiv:2412.05563*, 2024.

Adi Simhi, Itay Itzhak, Fazl Barez, Gabriel Stanovsky, and Yonatan Belinkov. Trust me, i'm wrong: High-certainty hallucinations in llms. *arXiv preprint arXiv:2502.12964*, 2025.

Lintang Sutawika, Leo Gao, Hailey Schoelkopf, Stella Biderman, Jonathan Tow, Baber Abbasi, ben fattori, Charles Lovering, farzanehnakhaee70, Jason Phang, Anish Thite, Fazz, Aflah, Niklas Muennighoff, Thomas Wang, sdtblck, nopperl, gakada, tttyuntian, researcher2, Chris, Julen Etxaniz, Zdeněk Kasner, Khalid, Jeffrey Hsu, AndyZwei, Pawan Sasanka Ammanamanchi, Dirk Groeneveld, Ethan Smith, and Eric Tang. Eleutherai/lm-evaluation-harness: Major refactor, December 2023. URL https://doi.org/10.5281/zenodo.10256836.

Mirac Suzgun, Nathan Scales, Nathanael Schärli, Sebastian Gehrmann, Yi Tay, Hyung Won Chung, Aakanksha Chowdhery, Quoc V Le, Ed H Chi, Denny Zhou, et al. Challenging big-bench tasks and whether chain-of-thought can solve them. *arXiv preprint arXiv:2210.09261*, 2022.

Gemma Team, Morgane Riviere, Shreya Pathak, Pier Giuseppe Sessa, Cassidy Hardin, Surya Bhupatiraju, Léonard Hussenot, Thomas Mesnard, Bobak Shahriari, Alexandre Ramé, et al. Gemma 2: Improving open language models at a practical size. *arXiv preprint arXiv:2408.00118*, 2024.

Gemma Team, Aishwarya Kamath, Johan Ferret, Shreya Pathak, Nino Vieillard, Ramona Merhej, Sarah Perrin, Tatiana Matejovicova, Alexandre Ramé, Morgane Rivière, et al. Gemma 3 technical report. *arXiv preprint arXiv:2503.19786*, 2025.

Roman Vashurin, Ekaterina Fadeeva, Artem Vazhentsev, Lyudmila Rvanova, Daniil Vasilev, Akim Tsvigun, Sergey Petrakov, Rui Xing, Abdelrahman Sadallah, Kirill Grishchenkov, et al. Benchmarking uncertainty quantification methods for large language models with lm-polygraph. *Transactions of the Association for Computational Linguistics*, 13:220–248, 2025.

Xi Wang, Laurence Aitchison, and Maja Rudolph. Lora ensembles for large language model fine-tuning. *arXiv preprint arXiv:2310.00035*, 2023.

Xuezhi Wang, Jason Wei, Dale Schuurmans, Quoc Le, Ed Chi, Sharan Narang, Aakanksha Chowdhery, and Denny Zhou. Self-consistency improves chain of thought reasoning in language models. *arXiv preprint arXiv:2203.11171*, 2022.

Jason Wei, Nguyen Karina, Hyung Won Chung, Yunxin Joy Jiao, Spencer Papay, Amelia Glaese, John Schulman, and William Fedus. Measuring short-form factuality in large language models. *arXiv preprint arXiv:2411.04368*, 2024.

Zhiqiu Xia, Jinxuan Xu, Yuqian Zhang, and Hang Liu. A survey of uncertainty estimation methods on large language models. *arXiv preprint arXiv:2503.00172*, 2025.

Yihao Xue, Kristjan Greenewald, Youssef Mroueh, and Baharan Mirzasoleiman. Verify when uncertain: Beyond self-consistency in black box hallucination detection. *arXiv preprint arXiv:2502.15845*, 2025.

An Yang, Baosong Yang, Beichen Zhang, Binyuan Hui, Bo Zheng, Bowen Yu, Chengyuan Li, Dayiheng Liu, Fei Huang, Haoran Wei, et al. Qwen2. 5 technical report. *arXiv preprint arXiv:2412.15115*, 2024.

Zhilin Yang, Peng Qi, Saizheng Zhang, Yoshua Bengio, William W Cohen, Ruslan Salakhutdinov, and Christopher D Manning. Hotpotqa: A dataset for diverse, explainable multi-hop question answering. *arXiv preprint arXiv:1809.09600*, 2018.

Lexin Zhou, Wout Schellaert, Fernando Martínez-Plumed, Yael Moros-Daval, Cèsar Ferri, and José Hernández-Orallo. Larger and more instructable language models become less reliable. *Nature*, 634(8032):61–68, 2024.

A Appendix

A.1 Theoretical Interpretations of Epistemic Uncertainty

Kernel and variational interpretation of $D(\omega \,||\, \omega^*)$. Assume the similarity function $s(\cdot,\cdot)$ is a symmetric positive definite kernel k. Denote the predictive distributions by $P_\Omega := p(\cdot \mid x;\omega)$ and P_{ω^*}. Their kernel mean embeddings in the reproducing kernel Hilbert space (RKHS) $\mathcal{H}_k$ are

$$\mu_\omega \;=\; \mathbb{E}_{r\sim P_\Omega}\big[k(r,\cdot)\big], \qquad \mu_{\omega^*} \;=\; \mathbb{E}_{q\sim P_{\omega^*}}\big[k(q,\cdot)\big].$$

Using the reproducing property $\langle k(r,\cdot), k(r',\cdot)\rangle_{\mathcal{H}_k} \;=\; k(r,r')$, the divergence in Eq. 2 can be rewritten exactly as:

$$D(\omega \,||\, \omega^*) = \langle \mu_\omega, \mu_\omega\rangle_{\mathcal{H}_k} \;-\; \langle \mu_\omega, \mu_{\omega^*}\rangle_{\mathcal{H}_k}. \tag{5}$$

Eq. 5 is the first two terms of the squared maximum mean discrepancy (MMD):

$$\mathrm{MMD}^2(P_\Omega, P_{\omega^*}) = \|\mu_\omega - \mu_{\omega^*}\|^2_{\mathcal{H}_k} = \underbrace{\|\mu_\omega\|^2_{\mathcal{H}_k} - \langle \mu_\omega, \mu_{\omega^*}\rangle_{\mathcal{H}_k}}_{D(\omega \,||\, \omega^*)} + \|\mu_{\omega^*}\|^2_{\mathcal{H}_k} - \langle \mu_\omega, \mu_{\omega^*}\rangle_{\mathcal{H}_k}.$$

Thus $D(\omega \,||\, \omega^*)$ is a *one-sided kernel discrepancy*: it measures how much the model's self-agreement exceeds its agreement with the ideal predictor, and it vanishes if and only if $\mu_\omega = \mu_{\omega^*}$ (and, for characteristic kernels, iff $P_\Omega = P_{\omega^*}$).

Variational-gap Interpretation. Write classical KL as $\mathrm{KL}(P_\Omega \,||P_{\omega^*}) = \mathrm{CE} - \mathrm{Ent}$, where $\mathrm{Ent} = \mathbb{E}_{r\sim P_\Omega}[-\log p(r \mid x;\omega)]$ and $\mathrm{CE} = \mathbb{E}_{r\sim P_\Omega}[-\log p(r \mid x)]$. Replacing $-\log$ with $-k$ yields

$$D(\omega \,||\, \omega^*) \;=\; \underbrace{\mathbb{E}_{r,r'\sim P_\Omega}[k(r,r')]}_{\text{“negative kernel-entropy”}} \;-\; \underbrace{\mathbb{E}_{r\sim P_\Omega,\, q\sim P_{\omega^*}}[k(r,q)]}_{\text{“kernel cross-entropy”}},$$

so D is the *semantic variational gap* between the model and the ideal distribution under the geometry induced by k. Minimizing D therefore projects P_Ω toward P_{ω^*} in RKHS while simultaneously penalizing model variability in P_Ω.

Lemma 1 (Bound on Kernel-Based Divergence)**.** *Let $P_\omega = p(\cdot \mid x,\omega)$ and $P_{\omega^*} = p(\cdot \mid x,\omega^*)$ be the predictive distributions of two language models. Let $k(\cdot,\cdot)$ be a symmetric, bounded, positive-definite kernel such that $0 \le k(r,r') \le 1$ for all r, r'. Define the kernel-based divergence*

$$D(\omega \,\|\, \omega^*) := \mathbb{E}_{r,r'\sim P_\omega}[k(r,r')] - \mathbb{E}_{r\sim P_\omega, q\sim P_{\omega^*}}[k(r,q)].$$

Then D is bounded above in absolute value by the total variation distance between P_ω and P_{ω^*}:

$$|D(\omega \,\|\, \omega^*)| \le \mathrm{TVD}(P_\omega, P_{\omega^*}),$$

where

$$\mathrm{TVD}(P_\omega, P_{\omega^*}) := \frac{1}{2}\int |p_\omega(z) - p_{\omega^*}(z)|dz.$$

Furthermore, if the RKHS norm of the embeddings are equal, i.e., $\|\mu_\omega\| = \|\mu_{\omega^*}\|$, then $D(\omega \,\|\, \omega^*) = 0$ implies $\mu_\omega = \mu_{\omega^*}$. If k is characteristic, this further implies $P_\omega = P_{\omega^*}$.

Proof. Define the kernel-smoothed function $f(z) := \mathbb{E}_{r\sim P_\omega}[k(r,z)]$. Then we can write

$$D(\omega \,\|\, \omega^*) = \mathbb{E}_{z\sim P_\omega}[f(z)] - \mathbb{E}_{z\sim P_{\omega^*}}[f(z)].$$

By the definition of total variation distance and the fact that $0 \le f(z) \le 1$ for all z,

$$|D(\omega \,\|\, \omega^*)| \le \sup_{\|f\|_\infty \le 1} |\mathbb{E}_{P_\omega}[f] - \mathbb{E}_{P_{\omega^*}}[f]| = \mathrm{TVD}(P_\omega, P_{\omega^*}).$$

For the second part, note that $D(\omega \,\|\, \omega^*) = \|\mu_\omega\|^2 - \langle \mu_\omega, \mu_{\omega^*}\rangle$. If $\|\mu_\omega\| = \|\mu_{\omega^*}\|$ and $D = 0$, then by Cauchy–Schwarz equality, we must have $\mu_\omega = \mu_{\omega^*}$. If the kernel is characteristic, then $\mu_\omega = \mu_{\omega^*}$ implies $P_\omega = P_{\omega^*}$. □

This result implies that $D(\omega \,\|\, \omega^*)$ provides a lower bound on distributional mismatch, and thus serves as a tractable proxy for epistemic uncertainty: it is provably small only when the model's predictive distribution aligns with that of the ensemble under the kernel geometry.

Under desired conditions mentioned in 3.2, and with a bounded characteristic kernel, $D(\omega \,||\, \omega^*) = 0$ if, and only if, the predictive distribution P_ω is close to the model set consensus as shown above. Consequently D (i) flags cases where the model's intra-model similarity is high (AU is low) while its agreement with the ensemble is low, (ii) rewards calibrated agreement by attaining its minimum only within the support of the ensemble, and (iii) remains sample-efficient, as it only requires $\mathcal{O}(n^2)$ kernel evaluations on n generated responses per model, which is cheaper than KL divergence evaluations or other approximations of EU.

A.2 Agreement and Coverage Metrics.

For every dataset we form the binary correctness matrix C_{ij} which is the correctness of response $r_i^{(j)}$ sampled from model j to input i, and compute two coarse descriptors of cross-model behaviour:

- **Jaccard redundancy** J – The mean pairwise Jaccard index of the sets of correctly answered examples:

$$J = \frac{2}{M(M-1)} \sum_{1 \le m < k \le M} \frac{|S_m \cap S_k|}{|S_m \cup S_k|}, \quad S_m = \{i : C_{im} = 1\}$$

  High J means models succeed on the same inputs.

- **Oracle-gain diversity** G – the additional coverage obtained by an oracle that chooses the correct model per example:

$$G = A_{\text{oracle}} - \max_m A_m = \frac{1}{N} \sum_{i=1}^{N} \mathbb{1}\left[\sum_{j=1}^{M} C_{ij} > 0\right] - \max_m \left(\frac{1}{N} \sum_{i=1}^{N} C_{im}\right)$$

  High G indicates that different models get different examples right.

A.3 Additional Experimental Setup

All experiments were conducted on two NVIDIA A100 80GB GPUs. We use the `lm-evaluation-harness` (Sutawika et al., 2023) codebase to generate responses from each model, and evaluate correctness using a local vLLM (Kwon et al., 2023) server hosting `Meta-Llama-3-70B-Instruct` (Grattafiori et al., 2024) as the judge model. Following prior work (Lin et al., 2023), we compute correctness using only the first sampled response from each model. All evaluation is conducted in inference-only mode; no training or fine-tuning is performed.

For each dataset, we sample 10 responses per model for the first 100 prompts. AU is computed using all 10 responses. To match the sample budget with TU, the experiments in Section 5.3 and Section 5.4 report results using only 2 responses per model for computing both TU and epistemic uncertainty. We use a temperature of 0.7 and top-p of 0.9 across all generations. For `SimpleQA`, model outputs are obtained from the OpenAI and Anthropic APIs.

Semantic similarity between responses is measured using cosine distance over `sentence-T5-xl` (Hou et al., 2022; Ni et al., 2021) embeddings. For datasets not originally supported by `lm-eval-harness`, we follow its prompt formatting conventions and include code for these additions in the supplementary material.

A.4 Additional Results on Total Uncertainty

Figure 8 reports the AUROC of aleatoric and total uncertainty across all model–dataset pairs, and Figure 9 shows the corresponding improvements from using TU over AU. Total uncertainty consistently improves correctness discrimination in nearly all cases, with the largest per-instance gains observed on `HotpotQA`, a benchmark known for complex multi-hop reasoning.

AUROC Results Per Model and Dataset. Figure 8 and Table 2 show AUROC of TU and AU in all model-dataset combinations, and Figure 9 shows the improvement of total uncertainty over AU in AUROC. TU improves AUROC in nearly all model–dataset combinations, with the largest gains observed in `HotpotQA`. Model performance substantially affects the magnitude of improvement. On datasets such as `XSum`, where overall model accuracy is low, TU yields large improvements for weaker models but occasionally underperforms for the strongest ones (e.g., `Llama` and `Qwen`), potentially due to disagreement with less reliable auxiliary models. A similar pattern holds on `GSM8K`, where gains are concentrated among lower-performing models, while others benefit less.

In contrast, `WMT16-de-en` and `CoQA` show limited gains, likely due to the high baseline accuracy ($> 90\%$) of all reference models (see Fig. 10), where AU is already well-calibrated. Notably, TU corrects miscalibrated AU for specific models, such as `Mistral` on `CoQA`, where the base AU is anomalously low. On `TruthfulQA`, which features open-ended questions with diverse valid answers, semantic disagreement does not reliably indicate epistemic uncertainty, which results in weaker improvements.

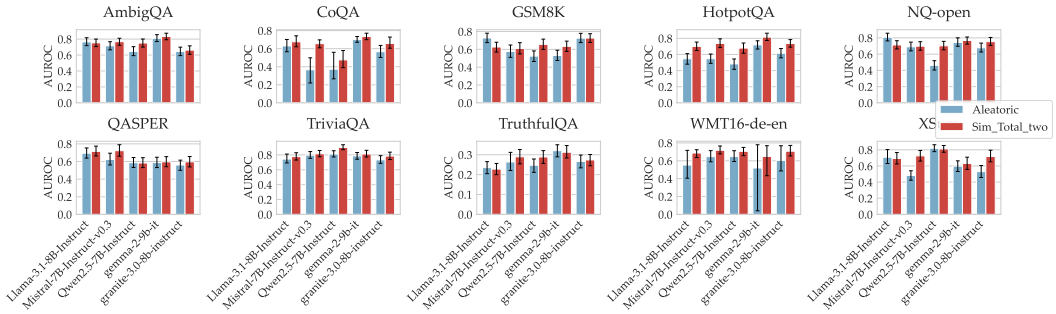

Figure 8: We show AUROC for each model separately to compare aleatoric and total uncertainty. TU consistently yields higher AUROC across models. We subsample 80% of the questions per dataset, 1000 times, to compute AUROC with 5% confidence intervals around the median AUROC value.

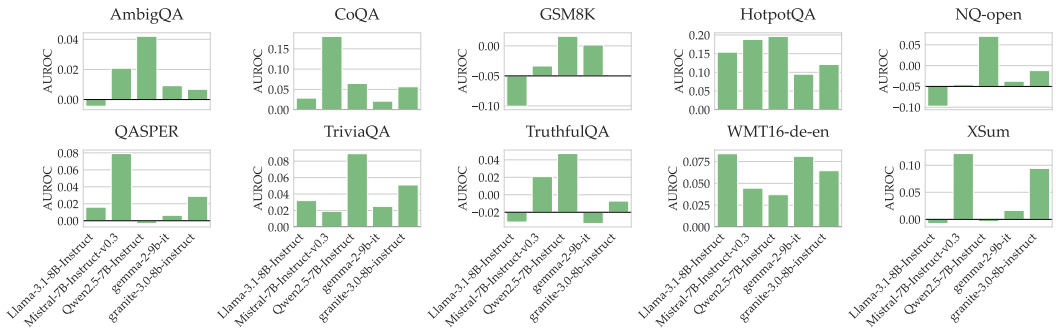

Figure 9: AUROC improvement obtained by adding EU to AU across all samples per dataset, measured as (Total − Aleatoric).

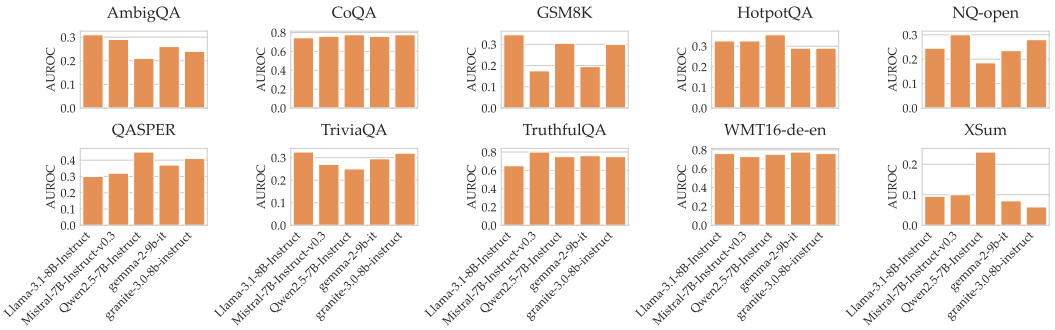

Figure 10: Accuracy per model-dataset pair.

ROC Curves. Figure 11 shows the ROC curve computed over the pooled set of all model–dataset pairs. TU achieves a higher AUROC (0.746 vs. 0.707), which shows improved seperation between correct and incorrect generations compared to AU alone. Figure 12 presents ROC curves for individual datasets. TU yields consistently better or comparable performance across all tasks, with the largest gains observed on `HotpotQA`, `WMT16-de-en`, and `CoQA`. These improvements align with our earlier findings that TU is most effective on tasks where models are accurate but occasionally confidently wrong.

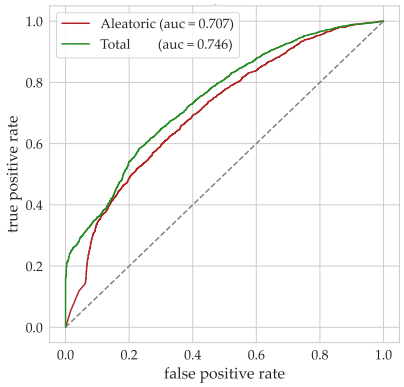

Figure 11: ROC curves between aleatoric and total uncertainty aggregated across all models and datasets. Total uncertainty achieves higher AUROC, indicating better discrimination between correct and incorrect generations.

Table 2: Uncertainty AUROC scores across models and benchmarks when different 7B/8B/9B parameter models are used as auxiliary models. Total Uncertainty is better calibrated with correctness than Aleatoric Uncertainty.

Benchmark	Model	Accuracy	Aleatoric AUROC	Epistemic AUROC	Total AUROC
AmbigQA	Llama-3.1-8B-Instruct	0.62	**0.764**	0.52	0.753
	Mistral-7B-Instruct-v0.3	0.58	0.716	0.506	**0.768**
	Qwen2.5-7B-Instruct	0.42	0.645	0.639	**0.75**
	gemma-2-9b-it	0.52	0.81	0.447	**0.833**
	granite-3.0-8b-instruct	0.48	0.644	0.488	**0.661**
CoQA	Llama-3.1-8B-Instruct	0.93	0.788	0.797	**0.845**
	Mistral-7B-Instruct-v0.3	0.95	0.458	0.80	**0.819**
	Qwen2.5-7B-Instruct	0.97	0.466	0.567	**0.595**
	gemma-2-9b-it	0.95	0.876	0.80	**0.918**
	granite-3.0-8b-instruct	0.97	0.708	**0.907**	0.821
GSM8K	Llama-3.1-8B-Instruct	0.69	**0.727**	0.346	0.626
	Mistral-7B-Instruct-v0.3	0.35	0.577	0.606	**0.61**
	Qwen2.5-7B-Instruct	0.61	0.524	0.623	**0.656**
	gemma-2-9b-it	0.39	0.531	0.601	**0.634**
	granite-3.0-8b-instruct	0.60	0.726	0.472	**0.727**
HotpotQA	Llama-3.1-8B-Instruct	0.65	0.546	0.662	**0.7**
	Mistral-7B-Instruct-v0.3	0.65	0.548	0.682	**0.736**
	Qwen2.5-7B-Instruct	0.71	0.483	**0.681**	0.679
	gemma-2-9b-it	0.58	0.719	0.608	**0.814**
	granite-3.0-8b-instruct	0.58	0.615	0.634	**0.736**
NQ-open	Llama-3.1-8B-Instruct	0.49	**0.808**	0.389	0.713
	Mistral-7B-Instruct-v0.3	0.60	0.69	0.501	**0.698**
	Qwen2.5-7B-Instruct	0.37	0.462	0.696	**0.703**
	gemma-2-9b-it	0.47	0.743	0.538	**0.768**
	granite-3.0-8b-instruct	0.56	0.678	0.541	**0.754**
QASPER	Llama-3.1-8B-Instruct	0.30	0.694	0.487	**0.714**
	Mistral-7B-Instruct-v0.3	0.32	0.623	0.657	**0.722**
	Qwen2.5-7B-Instruct	0.45	**0.587**	0.492	0.583
	gemma-2-9b-it	0.37	0.588	0.509	**0.596**
	granite-3.0-8b-instruct	0.41	0.56	0.512	**0.596**
TriviaQA	Llama-3.1-8B-Instruct	0.65	0.744	0.562	**0.776**
	Mistral-7B-Instruct-v0.3	0.54	0.796	0.552	**0.815**
	Qwen2.5-7B-Instruct	0.5	0.811	0.668	**0.9**
	gemma-2-9b-it	0.59	0.787	0.645	**0.812**
	granite-3.0-8b-instruct	0.64	0.733	0.575	**0.784**
TruthfulQA	Llama-3.1-8B-Instruct	0.65	**0.47**	0.423	0.456
	Mistral-7B-Instruct-v0.3	0.80	0.528	**0.601**	0.579
	Qwen2.5-7B-Instruct	0.75	0.494	**0.584**	0.578
	gemma-2-9b-it	0.76	**0.641**	0.541	0.625
	granite-3.0-8b-instruct	0.75	0.532	**0.556**	0.548
WMT16-de-en	Llama-3.1-8B-Instruct	0.95	0.691	0.695	**0.859**
	Mistral-7B-Instruct-v0.3	0.91	0.808	0.835	**0.897**
	Qwen2.5-7B-Instruct	0.94	0.809	0.832	**0.883**
	gemma-2-9b-it	0.97	0.649	0.663	**0.811**
	granite-3.0-8b-instruct	0.95	0.755	0.493	**0.884**
XSum	Llama-3.1-8B-Instruct	0.19	**0.708**	0.37	0.693
	Mistral-7B-Instruct-v0.3	0.20	0.482	0.651	**0.725**
	Qwen2.5-7B-Instruct	0.48	**0.819**	0.31	0.811
	gemma-2-9b-it	0.16	0.598	0.565	**0.631**
	granite-3.0-8b-instruct	0.12	0.529	0.582	**0.717**

Comparison with Baselines. We compare TU against a number of baselines: Mean Token Entropy (Fomicheva et al., 2020), Maximum Token Probability (Fadeeva et al., 2023), Maximum Sequence Probability (Fadeeva et al., 2023), Perplexity (Fomicheva et al., 2020), PTrue (Kadavath et al., 2022), Self-Certainty (Kang et al., 2025), Semantic Entropy (Kuhn et al., 2023a), SC (Self-Consistency) Score (Wang et al., 2022; Manakul et al., 2023), SelfCheckGPT (Manakul et al., 2023), Kernel Language Entropy (Nikitin et al., 2024), Closeness Centrality, SC + VC (Verbalized confidence), and SC based CV (Jiang et al., 2024). We use implementations from Fadeeva et al. (2023); Jiang et al. (2024). AU baselines is the same as (Lin et al., 2023), but instead of using entailment with Deberta to compute response sequence similarity, we use a `sentence-T5-xl` model. Results are provided in Table 3.

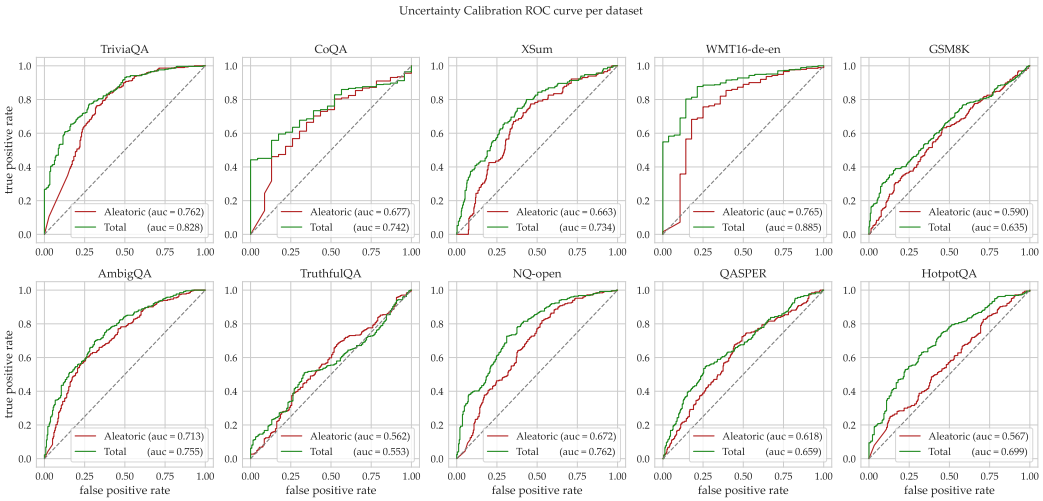

Figure 12: ROC curves comparing aleatoric and total uncertainty across individual datasets. TU achieves higher AUROC across most tasks, particularly on `HotpotQA`, `WMT16-de-en`, and `CoQA`, where models exhibit confident failures.

Table 3: Uncertainty AUROC scores across benchmarks for `Mistral-7B` when different 7B/8B/9B parameter models are used as auxiliary models. Total Uncertainty is better calibrated with correctness than Aleatoric Uncertainty and other baselines.

	AmbigQA	CoQA	GSM8K	HotpotQA	NQ-open	QASPER	TriviaQA	TruthfulQA	**Average**
Total	**0.768**	**0.819**	0.61	0.736	**0.698**	**0.722**	**0.815**	0.579	**0.718**
Aleatoric	0.716	0.458	0.577	0.548	0.69	0.623	0.796	0.528	0.617
Closeness Centrality	0.683	0.612	0.56	**0.739**	0.597	0.579	0.702	**0.639**	0.639
SC Score	0.649	0.553	0.551	0.711	0.616	0.567	0.673	0.603	0.615
SC Based VC	0.658	0.483	0.555	0.677	0.63	0.568	0.706	0.602	0.61
SemanticEntropy	0.678	0.561	0.584	0.526	0.656	0.514	0.637	0.514	0.584
SC + VC	0.671	0.411	0.544	0.51	0.641	0.581	0.731	0.581	0.584
Max Sequence Prob.	0.651	0.561	0.496	0.556	0.64	0.48	0.66	0.534	0.572
Mean Token Entropy	0.654	0.498	0.461	0.559	0.674	0.481	0.696	0.544	0.571
Token Entropy	0.654	0.502	0.465	0.558	0.672	0.481	0.69	0.542	0.57
Perplexity	0.661	0.513	0.462	0.548	0.652	0.464	0.672	0.527	0.562
Max Token Prob.	0.658	0.51	0.464	0.546	0.652	0.468	0.674	0.528	0.562
Self Certainty	0.569	0.51	0.459	0.553	0.598	0.484	0.63	0.586	0.549
PTrue	0.604	0.555	0.371	0.417	0.55	0.423	0.519	0.451	0.486
SelfCheckGPT	0.733	0.454	**0.77**	0.5262	0.688	0.619	0.667	0.534	0.603
Kernel Lang. Ent.	0.785	0.642	0.637	0.491	0.585	0.573	0.723	0.637	0.634

Correlation with BLEU and ROUGE. For the two generative tasks (`WMT16-de-en` and `XSum`), we additionally evaluate the correlation between uncertainty scores and standard automatic metrics (BLEU for translation, ROUGE for summarization). As shown in Table 4, both AU and TU show a moderate negative correlation with BLEU on `WMT16-de-en`, consistent with higher uncertainty aligning with lower translation quality. On `XSum`, AU shows a positive correlation with ROUGE, while EU exhibits a negative correlation (-0.213), which suggests that EU is a better proxy for quality degradation in summarization than AU in this setting.

Table 4: Pearson correlation between uncertainty scores and automatic evaluation metrics (BLEU for `WMT16-de-en`, ROUGE for `XSum`).

Dataset	**Metric**	**Aleatoric**	**Epistemic**	**Total**
`WMT16-de-en`	BLEU	-0.319	-0.115	-0.324
`XSum`	ROUGE	+0.162	-0.213	-0.056

A.5 The Effect of the Auxiliary Model Set on Total Uncertainty

Ablating the Reference Model Size. We test how the quality of total uncertainty estimates depends on the capability of the *reference model*, whose uncertainty we aim to estimate. We fix the auxiliary model set to a pool of four 7-9B models mentioned in 4 that are not from the same family as the reference model, and vary the reference model's architecture and size. Figure 13 reports results on `TriviaQA`, using two model families (`Gemma3` (Team et al., 2025) and `Qwen2.5` (Yang et al., 2024)) of various sizes. As the size of the reference model increases, both aleatoric and total uncertainty AUROC scores tend to decrease, but total uncertainty has consistently higher AUROC across different model sizes. This holds even when the reference model is substantially stronger than any model in the auxiliary set (e.g., `Qwen2.5-32B` vs. 7-9B peers).

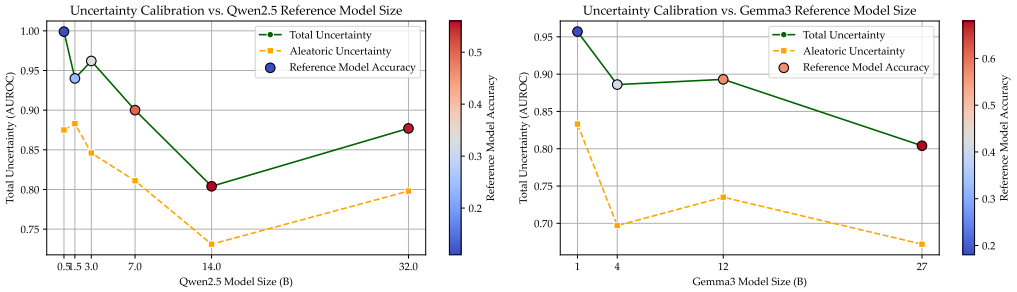

Figure 13: We vary the size of the **reference model** while holding the auxiliary models fixed. TU achieves higher AUROC in comparison to AU acorss different model sizes on `TriviaQA`.

Noise-perturbed Auxiliary Model Set. We consider noise-perturbed variants of the reference model itself as auxiliary model set, similar to Liu et al. (2025). Specifically, we apply a perturbation strategy in which we preserve the top-k singular vectors of each linear weight matrix and inject Gaussian noise into the remaining lower-rank subspace. This preserves dominant components of the model while allowing for controlled noise in its response distribution. Figure 14 in the appendix shows that the we sometimes obtain improvement in TU-AU, but it is overall lower than for the more diverse auxiliary model set from Figure 4.

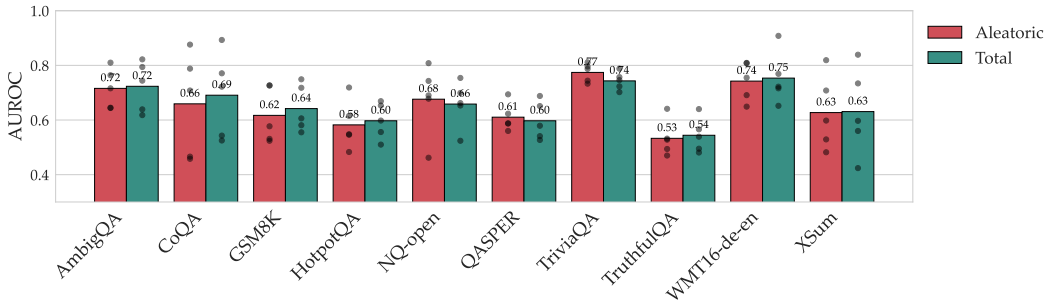

Figure 14: Uncertainty calibration for experiments where auxiliary model set for each model is consisted of multiple noise-perturbed models

A.6 Ablations

Number of Auxiliary Models. We study how the size of the auxiliary model set affects the quality of total uncertainty estimates. For each reference model, we compute total uncertainty using $n \in \{2, 3, 4, 5\}$ models, where one model is fixed (the reference model) and the remaining $n - 1$ are sampled from other model families. All methods use a fixed number of samples per model.

Figure 15 shows that total uncertainty improves monotonically as the number of auxiliary models increases. This holds across almost all tasks, with the largest gains typically occurring between $n = 2$

and $n = 3$. In addition, we observe that variance across runs decreases as more models are added, which suggests a more calibrated uncertainty score can be achieved from increasing the number of model in the auxiliary set. However, in all datasets, our multi-sample total uncertainty measure outperforms aleatoric uncertainty in AUROC, even when only one auxiliary model is used.

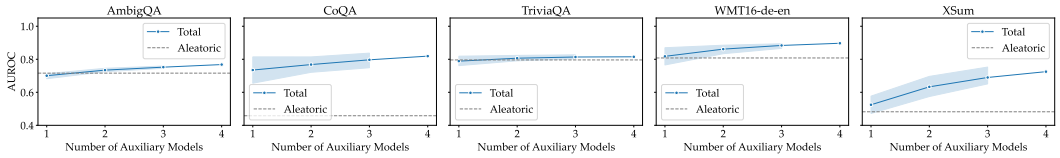

Figure 15: We plot AUROC as a function of the number of auxiliary models used to compute total uncertainty for `Mistral-7B-Instruct-v0.3`. Total uncertainty improves with more models, and variance decreases.

Number of Samples for Uncertainty Estimation. We next investigate how the number of response samples per model affects the performance of uncertainty estimates. For each model in the auxiliary set, we vary the number of generations used in total uncertainty computation from 5 to 50, and compare against two baselines for aleatoric uncertainty: one computed using 5 samples and another using 10 samples, matching the regimes used in our main experiments.

As shown in Figure 16, AUROC for total uncertainty usually slightly increases with more samples, with diminishing returns beyond 30 samples in most tasks. Notably, TU consistently outperforms AU baselines across all datasets. These findings also reinforce the practicality of TU even under constrained budgets, as improvements are apparent with as few as 10 samples ($n = 5$ on the x-axis).

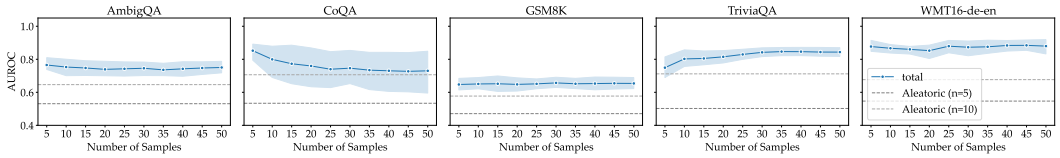

Figure 16: AUROC of total uncertainty as a function of the number of samples per model. Even with a small number of samples, TU outperforms aleatoric baselines (5-sample and 10-sample variants). Gains saturate around 30–40 samples.

Similarity Backbone. To test the robustness of our results to the choice of similarity function, we repeated the analysis on `TriviaQA` using `deberta-large-mnli` (entailment probability as similarity) in addition to the original `sentence-T5-xl` embeddings. As shown in Table 5, the performance trend (TU > AU) remains consistent across both similarity measures, which confirms that our framework is not dependent on a specific similarity backbone.

Table 5: AUROC on `TriviaQA` using two different similarity backbones: cosine similarity over `sentence-T5-xl` embeddings vs. entailment probability from `deberta-large-mnli`. TU consistently outperforms AU regardless of the similarity measure.

	Embedding (sentence-T5-xl)		**Entailment (deberta-large-mnli)**	
Model	AU	TU	AU	TU
`Mistral-7B-Instruct-v0.3`	0.796	0.815	0.788	0.885
`Qwen2.5-7B-Instruct`	0.811	0.900	0.801	0.905
`granite-3.0-8b-instruct`	0.733	0.784	0.740	0.821
`Llama-3.1-8B-Instruct`	0.744	0.776	0.752	0.810
`gemma-2-9b-it`	0.787	0.812	0.765	0.862

Weighted Total Uncertainty. Our formulation defines $TU = AU + EU$ (Equation 4). In practice, one could also consider a weighted interpolation $TU_\lambda = \lambda \cdot U_{\text{aleatoric}} + (1 - \lambda) \cdot U_{\text{epistemic}}$, where λ controls the relative contribution of each component. Note that we do not assume access to

correctness labels at uncertainty quantification time, so λ is not tuned as a hyperparameter. Table 6 reports AUROC across all benchmarks (averaged over five reference models) for different values of λ. While specific values of λ can yield marginal gains on individual datasets, the unweighted sum (TU) consistently outperforms AU across all benchmarks without requiring task-specific calibration.

Table 6: AUROC for weighted total uncertainty $TU_\lambda = \lambda \cdot AU + (1 - \lambda) \cdot EU$ across benchmarks, averaged over five reference models. Bold indicates the best score per dataset. The unweighted TU (= AU + EU) is competitive across all benchmarks without requiring tuning.

Metric	AmbigQA	CoQA	GSM8K	HotpotQA	NQ-open	QASPER	TriviaQA	TruthfulQA	WMT16	XSum
AU	0.716	0.659	0.617	0.582	0.676	0.610	0.774	0.533	0.315	0.603
EU	0.520	0.774	0.529	0.654	0.533	0.531	0.600	0.541	0.384	0.527
TU	0.753	0.800	**0.651**	0.733	0.727	**0.642**	0.817	0.557	0.384	**0.707**
λ=0.1	0.556	0.792	0.549	0.676	0.565	0.548	0.648	0.546	0.384	0.543
λ=0.2	0.599	0.803	0.575	0.698	0.603	0.576	0.699	0.555	**0.386**	0.568
λ=0.3	0.661	**0.825**	0.597	0.725	0.646	0.602	0.752	0.562	**0.386**	0.612
λ=0.4	0.714	0.818	0.628	**0.744**	0.689	0.631	0.795	**0.563**	0.383	0.679
λ=0.5	0.753	0.800	0.651	0.733	0.727	0.642	0.817	0.557	0.384	0.707
λ=0.6	**0.764**	0.777	0.648	0.701	**0.739**	0.639	**0.825**	0.549	0.379	0.678
λ=0.7	0.754	0.751	0.639	0.662	0.731	0.635	0.823	0.547	0.365	0.649
λ=0.8	0.742	0.726	0.628	0.634	0.713	0.627	0.812	0.545	0.352	0.627
λ=0.9	0.732	0.708	0.624	0.611	0.695	0.621	0.799	0.537	0.333	0.613

A.7 Additional Results on Multiple-choice QA tasks

To evaluate whether our findings extend beyond open-ended generation, we adapt a subset of tasks from the Big-Bench Hard (BBH) (Suzgun et al., 2022) benchmark into a long-form QA format with chain-of-thought answering. Specifically, we consider `Boolean Expressions`, `Disambiguation QA`, and `Word Sorting`, and prompt models to justify their answers rather than selecting from multiple choices directly. We then evaluate uncertainty scores over the full responses using the same semantic similarity pipeline as in our main experiments.

Table 7 reports AUROC scores for both AU and TU across models on these tasks. We observe that TU improves over AU in most cases, with the largest gains appearing when base model performance is low (e.g., Qwen2.5-7B on `Disambiguation QA` and `Boolean Expressions`). These results demonstrate that TU remains effective in identifying incorrect generations even when the task is originally framed as multiple-choice, provided responses are elicited in free-form.

Table 7: Uncertainty AUROC scores across models and benchmarks when different 7B/8B/9B parameter models are used as auxiliary models. Total Uncertainty is better calibrated with correctness than Aleatoric Uncertainty.

Benchmark	Model	**Accuracy**	**Aleatoric AUROC**	**Total AUROC**
BBH Fewshot Boolean Expressions	Llama-3.1-8B-Instruct	**0.88**	**0.662**	0.658
	Mistral-7B-Instruct-v0.3	**0.84**	**0.746**	0.735
	Qwen2.5-7B-Instruct	**0.53**	0.744	**0.909**
	gemma-2-9b-it	**0.86**	0.593	**0.725**
	granite-3.0-8b-instruct	**0.9**	**0.659**	0.658
BBH Fewshot Disambiguation QA	Llama-3.1-8B-Instruct	**0.59**	0.544	**0.594**
	Mistral-7B-Instruct-v0.3	**0.64**	0.525	**0.656**
	Qwen2.5-7B-Instruct	**0.44**	0.561	**0.81**
	gemma-2-9b-it	**0.69**	0.61	**0.65**
	granite-3.0-8b-instruct	**0.62**	0.486	**0.562**
BBH Fewshot Word Sorting	Llama-3.1-8B-Instruct	**0.69**	0.476	**0.512**
	Mistral-7B-Instruct-v0.3	**0.77**	**0.529**	0.429
	Qwen2.5-7B-Instruct	**0.44**	0.587	**0.645**
	gemma-2-9b-it	**0.96**	0.475	**0.576**
	granite-3.0-8b-instruct	**0.58**	**0.578**	0.485

A.8 Epistemic Uncertainty Analysis

Figure 17 disaggregates the trend shown in Figure 2a by model. For all five reference models, incorrect generations in the low-AU regime show consistently higher EU than correct ones, which reaffirms that EU captures confident failures missed by self-consistency. This separation weakens in mid- and high-AU buckets, where both correct and incorrect outputs tend to be more uncertain. The consistency of this pattern across different models highlights the effectiveness of EU in identifying unreliable predictions when AU alone is low. Similarly, Figure 18 shows a similar trend when results are disaggregated by *dataset*.

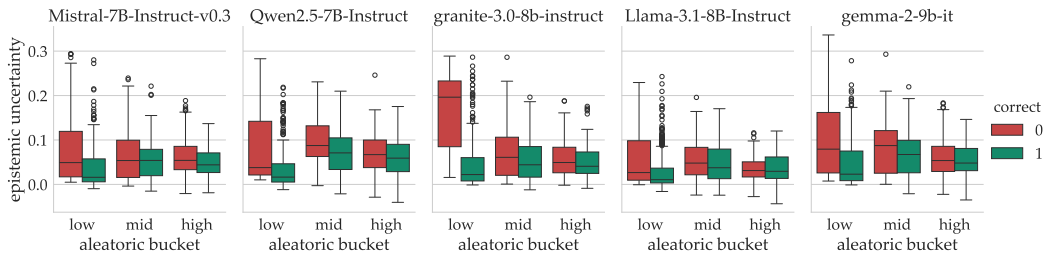

Figure 17: Distribution of EU across different levels of AU and correctness. Across all models, we find that incorrect responses in the low-aleatoric regime are assigned higher EU than correct ones on average.

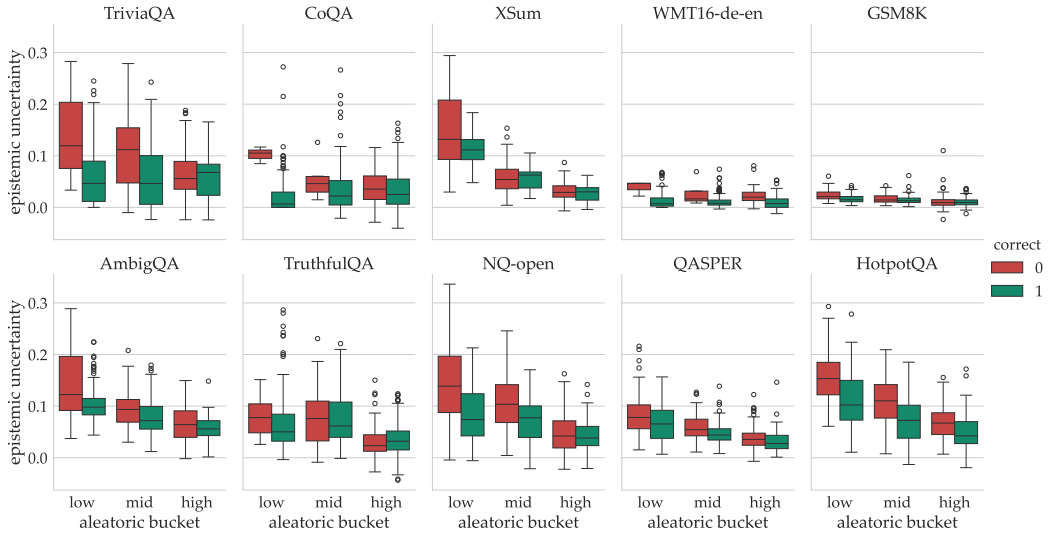

Figure 18: Distribution of EU across different levels of AU and correctness. Across all benchmarks, we find that incorrect responses in the low-aleatoric regime are assigned higher EU than correct ones on average.

A.9 Computational cost

We report full wall-clock measurements to contextualize the overhead introduced by our TU ensemble relative to a self-consistency baseline with the same total sample budget. All runs use **TriviaQA** on a single Nvidia L40S (48 GB) unless noted. Decoding settings and similarity-oracle calls are identical across settings; the observed gap comes from loading additional checkpoints.

Takeaways. 1) *Token-generation and similarity costs are matched* between the self-consistency baseline (1×10 samples) and TU (5×2). 2) *Sequential overhead is dominated by checkpoint loads*; peak VRAM does not increase. 3) *Parallel execution amortizes loading*: with $5\times$ parallelism, TU matches single-model wall-clock while retaining its AUROC and selective-abstention improvements.

Regime	Setting	Models × samples	Per-model mean (s)	Total wall-clock (s)
Single-GPU (sequential)	Single model, 10 samples	$1 \times$ 7–9B $\times$ 10	244.1 ± 58.7	244.1
Single-GPU (sequential)	TU ensemble, 5 models $\times$ 2 samples	$5 \times$ 7–9B $\times$ 2	78.3 ± 12.9	391.7
Multi-GPU (parallel, 5×)	TU ensemble, 5 models $\times$ 2 samples	$5 \times$ 7–9B $\times$ 2	78.3 ± 12.9	≈ 78

Table 8: **Wall-clock on TriviaQA.** Sequential TU is slower due to streaming four extra checkpoints; peak GPU memory is unchanged. With 5-way parallelism (one GPU per model), wall-clock returns to $\sim$78 s while preserving TU's calibration and abstention gains.

In practice, a small ensemble (2–5 auxiliaries, 1–2 samples each) provides most of the TU benefit under common deployment envelopes.

Computational overhead of loading models. We acknowledge the higher memory requirement of loading multiple models but emphasize that our comparison controls for total inference compute budget. Specifically, our main results compare AU (10 samples) against TU (2 samples $\times$ 5 models), which keeps the total tokens generated the same.

This overhead is a tradeoff for better UQ, because increasing the sampling budget for the single-model baseline does not close the performance gap. As shown in Table 9, increasing the sampling budget for AU from 5 to 20 does not improve AUROC for AU. In contrast, TU with just 5 total samples (1 sample $\times$ 5 models) consistently outperforms AU with 20 samples.

Table 9: AUROC on `TriviaQA` under varying sampling budgets. Increasing AU samples does not close the gap with TU.

Model	**AU** n=5	**AU** n=10	**AU** n=15	**AU** n=20	**TU** n=1×5	**TU** n=2×5
`Llama-3.1-8B-Instruct`	0.78	0.78	0.82	0.81	0.89	0.87
`Mistral-7B-Instruct-v0.3`	0.71	0.74	0.76	0.76	0.87	0.85
`Qwen2.5-7B-Instruct`	0.78	0.83	0.84	0.84	0.93	0.92
`gemma-2-9b-it`	0.70	0.70	0.71	0.71	0.84	0.83
`granite-3.0-8b-instruct`	0.73	0.72	0.74	0.74	0.90	0.89

This confirms that the confident failures we found are systematic, and these models often have collapsed posteriors on incorrect answers, so oversampling cannot recover the uncertainty. The ensemble overhead provides qualitatively new information (cross-model disagreement) that is inaccessible to single models.

A.10 Computing Correctness Using an LLM Judge

We compute correctness scores using `Meta-Llama-3-70B-Instruct` deployed via a local `vLLM` server. Each model prediction is evaluated independently against the gold answers using a structured prompt that includes five few-shot examples, held fixed across all evaluations. The prompt instructs the judge to assign a correctness score from the discrete set `{0.0, 0.1, ..., 1.0}` based on the alignment between the predicted and gold answers, while explicitly ignoring the model's own knowledge.

The judge receives as input: (1) the user-defined task or question, (2) a list of gold answers, and (3) the model-generated answer. It is instructed to output a JSON object containing a numerical score and a justification. The request is submitted using deterministic decoding (`temperature`= 0, `max_tokens` = 20), and we employ up to three retries with truncated context in case of failures due to prompt length.

Correctness is evaluated using the first response generated by each model. The gold answers are passed verbatim, and no normalization is applied to either predictions or references. By default, a prediction is considered correct if its score exceeds 0.5. For tasks where differences should be penalized (e.g., summarization or translation), we increase the threshold to 0.9 (specifically, for `XSum` and `WMT16-de-en`). These thresholds are applied during AUROC and selective prediction evaluations.

Judge Evaluation. We assess the reliability of the LLM judge used to score correctness against gold references. First, we perform a cross-judge check (Llama-3-70B-Instruct vs. GPT-4o) and find high agreement on both probabilities and binary labels. In 93/100 cases the judges produced identical correctness probabilities. In 5/100, probabilities differed but mapped to the same binary label under the 0.5 threshold, so AUROC is unchanged. Only 2/100 items were hard conflicts, and manual inspection favored GPT-4o in both.

Second, We manually audited 100 Mistral-generated samples across TriviaQA and TruthfulQA and observed <6% human–judge disagreement. We also compare to rule-based matchers from `lm-evaluation-harness` and find them brittle for free-form outputs, which motivagtes an LLM judge.

Prompt Format. We provide the prompt format used for the LLM Judge here.

```
I want you to act as a judge for how well a model did answering a
user-defined task.
You will be provided with a user-defined task that was given to the
model, its golden answer(s), and the model's answer.  The context of
the task may not be given here.  Your task is to judge how correct
the model's answer is based on the golden answer(s), without seeing
the context of the task, and then give a correctness score.  The
correctness score should be one of the below numbers:  0.0 (totally
wrong), 0.1, 0.2, ..., 1.0 (totally right).  You should also add a
brief justification regarding how the model's answer conforms to
or contradicts the golden answer(s).  Your response must follow the
format:
{
"correctness_score":  your_score,
"justification":  your_justification
}
Note that each one of the golden answers is considered correct.  Thus
if the model's answer matches any one of the golden answers, it should
be considered correct.
--
Example 1:
User-defined task -- Sandy bought 1 million Safe Moon tokens.  She has
4 siblings.  She wants to keep half of them to herself and divide the
remaining tokens among her siblings.  After splitting it up, how many
more tokens will she have than any of her siblings?
Golden Answer(s) -- <answer 1> 375000
Model's Answer -- Sandy will have more tokens than any sibling by 3/8
million.
Model Output:
{
"correctness_score":  1.0,
"justification":  "The model's answer of 3/8 million equals 375,000,
which matches the gold answer exactly."
}
--
...  (3 more examples)
--
Target Example:
User-defined task -- [QUESTION]
Golden Answer(s) -- <answer 1> [...]; <answer 2> [...]
Model's Answer -- [MODEL RESPONSE]
Model Output:
{
"correctness_score":  ?,
"justification":  ?
}
```